

# Tensile and Shear Experiments using Polypropylene/Polyethylene Foils at different Temperatures

C. Sguazzo, St. Hartmann

*An experimental campaign on a thermo-plastic copolymer of polypropylene/polyethylene (PP/PE) serves to investigate the rate- and temperature-dependence of the material. Isothermal tensile and shear experiments for four different constant displacement-rates and temperatures ( $-10\text{ }^{\circ}\text{C}$  -  $120\text{ }^{\circ}\text{C}$ ) are conducted, monitored by means of a Digital Image Correlation (DIC) system. The tensile experiments are carried out within the large deformation range, where localization phenomena are observed. This requires the application of a full-field deformation analysis system to develop stress-stretch (strain) diagrams, which are necessary with regard to aspects of constitutive modeling. In addition to these experiments, a modified three-rail shear tool was designed in order to investigate the shear behavior of PP/PE. Apart from the rate-dependence, the relaxation behavior is investigated for both tensile and shear load conditions by means of multi-step relaxation tests at different temperatures in order to obtain indications about the equilibrium stress state of the material.*

## 1 Introduction

There are modern process technologies involving multi-layered steel-polymer-steel composites, in which the polymer layer is used for damping purposes - see, for example, (Lange et al., 2009), or, (Palkowski et al., 2013). In order to understand and predict the forming process of a sandwich laminate, for instance, in the scope of a deep drawing process, knowledge about the polymer's material behavior is essential. In this investigation, we focus on polypropylene/polyethylene (PP/PE) foils. Since there are different temperatures in the production process and in everyday applications, we investigate the material behavior under different temperatures. In a first step, we choose constant temperatures levels to study the mechanical behavior under constant temperature conditions. Thus, temperature-rate dependence is out of the scope of these preliminary investigations.

For many decades, thin-foil thermo-plastic polymers have been employed within more complex composite structures. In the automotive field, they are commonly used as the inner core of multi-layered sandwich materials with an external skin of steel. When subjected to forming processes, both the external layers and the inner core polymer layer undergo large deformations. Consequently, an extensive analysis of the mechanical characteristics of the polymer is required within such a range of deformation.

It is also necessary to investigate the temperature-influence, because the production process of layered composites is characterized by high temperatures ( $120\text{ }^{\circ}\text{C}$ ), necessary for activating the epoxy resin which bonds the steel and the polymer layers. Furthermore, the sandwich material structure is used in cars and during its service life, i.e. it is exposed to temperatures above and below room temperature of  $20\text{ }^{\circ}\text{C}$ .

The thermo-plastic copolymer, which is object of the present experimental investigation, is a blend of polypropylene and polyethylene with talc, rutile and barite fillers. It is provided in the form of a thin layered material. Thermo-plastic polymers, with regard to a single material or to a blend, have been studied for many decades, with particular attention to the influence of the testing rate and to its coupled effects with the temperature.

Since thermo-plastics are employed in numerous industrial applications and technologies, there is a wide range of theoretical and experimental scientific literature, ranging from the research fields of Material Science, Chemistry and Physics to Continuum Mechanics. In the following, we provide a brief overview of the research background. The present work aims to contribute to this field by focusing on the thermo-mechanical properties of the PP/PE material that are necessary to develop a material model by means of a continuum mechanical approach.

The yielding of glassy polymers has been presented in early work by Argon (1973). It models the intermolecular

interactions and interprets the macroscopic plastic deformation of glassy polymers. It considers the division of the plastic resistance of a polymer into a part depending on the pressure, the temperature and the strain-rate and a part depending on the stretch. The theory was developed for the first part and applied to initially un-oriented isotropic polymers.

The conventional methods of tensile testing applied to polymers were reviewed by G'Sell and Jonas (1979), who analyzed the features of both displacement-rate and strain-rate experiments and pointed out that a larger variation of local strain-rate occurs when necking takes place. Flow curves for high density polyethylene and polyvinyl chloride have been determined at room temperature over four orders of magnitude of strain-rates. A constitutive relation has been developed for the flow curves, which considers a bigger role considering that the aspect of the localization plays a more important role with respect to the rate-sensitivity. The mechanical behavior of high and low density polyethylene and polypropylene dumbbell specimens, together with other polymers, were also investigated by G'Sell and Jonas (1981). They performed tensile tests at room temperature and constant local true strain-rates, and they investigated the influence of the strain-rate change on the transient and the yield behavior of the polymers. Furthermore G'Sell et al. (1992) and G'Sell et al. (2002) developed and improved a tensile testing method to determine the plastic behavior of polymers under tension and within the large deformation range, where necking phenomena occur. Thanks to such a technique, it was possible to evaluate the stress-strain behavior and to determine the volume strain at a constant true strain.

The large strain deformation response of glassy polymers under uniaxial compression load conditions have been widely investigated by Arruda et al. (1995) and Zaroulis and Boyce (1997). By varying the strain-rate and the temperature during the tests, it was found out that initial yield is dependent on these factors. Furthermore, the rate-dependence of the strain softening and the strain hardening was found to be strictly coupled to the temperature. At moderate strain-rates, in fact, the temperature rises due to the deformation heating and this mechanism has significantly more influence at high rates than it has at low strain-rates. A drastic softening of the stress-strain behavior of the polymer material has also been observed in connection with an increase of temperature.

A substantial review of the mechanical response of glassy polymers during relaxation processes is presented in (Haward and Young, 1997), including investigations of the post-yield behavior and the influence of thermal effects. There are only a few experimental studies in which the mechanical properties of blends of polyethylene and polypropylene were determined by means of tensile tests. In (Lovinger and Williams, 1980) the yield stress and the tensile modulus of different combinations of polypropylene and polyethylene were found to increase with the proportion of polypropylene. More recently, Drozdov et al. (2010) investigated the strain-rate and the relaxation behavior of binary blends of metallocene catalyzed polypropylene and low density polyethylene at room temperature, confirming an increase of the yield stress with the polypropylene ratio.

Maher et al. (1980) studied the development of heat during the formation of necking, observing that the amount of heat loss varies with the speed at which the experiment is performed. Further, they introduced an equation to obtain the locally developed maximum temperature at each testing rate.

The more recent scientific literature in this scope is primarily characterized by studies of the mechanical characteristics of thermo-plastics together with the analysis of the strain field by means of digital image correlation (DIC). Grytten et al. (2009) used a DIC-system to study a talc and elastomer modified polypropylene compound subjected to large strains during tensile experiments, proposing two procedures to calculate the true stress-strain relations. De Almeida et al. (2008) developed an optical device, based on a DIC-system, in order to obtain the strain behavior in thickness direction of a polypropylene/EPR/talc composite and to evaluate the volumetric deformation gradients, excluding the assumptions of classical incompressibility and isotropy. Maurel-Pantel et al. (2015) investigated the mechanical behavior and the thermo-mechanical coupling of polyamide within the large deformation range, of tensile and shear loading by means of a DIC-system. An overview of the DIC-system is given in (Sutton et al., 2009).

In order to obtain additional information concerning the behavior of PP/PE, the study of the mechanical properties under shear conditions is also of main interest. Different possibilities of performing in-plane shear tests with thin layered materials - such as metals, composites and polymers, and consequently, with different specimen geometries - can be found in the technical standards and in the scientific literature. The rail shear method, described in (ASTM D4255/D4255M-15a, 2015) and (ASTM D7078/D7078M-12, 2012), consists of a tool that is inserted in a tensile testing machine in order to obtain conditions of plane shear by means of the vertical movement of the tool. The two possible existing configurations are based on an upper and a lower part, including two or three rails, that are connected to the tensile testing machine. The sample is inserted into the space between the rails. The three-rail arrangement, specifically, features two outer rails and an intermediate rail. The advantage of

such a configuration is that the specimen, clamped to all three rails, is subjected to symmetrically shear-loaded areas when the vertical displacement is applied, i.e. the bending influence is minimized. The Iosipescu test is another method for in-plane shear tests, originally developed for metals (Iosipescu, 1967) and later standardized for fiber composites (ASTM D5379/D5379M-12, 2012). The test arrangement is mounted into a compression testing machine, where one clamping moves in vertical direction and the other part is fixed, so that the notched specimen is sheared. In the panel shear test (ASTM D 2719), a flat sample is clamped into the frame, which is connected to a tensile testing machine. When the tensile load is applied, the shear stress state leads to a diamond-shaped deformed specimen. The maximum possible shear of the sample is limited by the small area clamped into the frame. One of the first approaches to determine the plastic behavior of thin polymer layers, including polyethylene material, by means of a rail test was presented by G'Sell and Boni (1983), who proposed a tool for plane shear experiments and investigated the strain hardening under simple shear conditions. Detailed comparisons of the existing techniques are presented in (Lee and Munro, 1986) and more recently in (Yin et al., 2014), where strain distribution measurements by means of DIC-systems are investigated too. There are also a few recent studies focusing on the analysis of the strain field under shear conditions by means of a DIC-system. The strain field developed by means of a rail shear tool within woven composite has been investigated for notched and un-notched specimens in (Rouault et al., 2013). A DIC-system was also employed for testing three different polypropylene-based materials in (Daiyan et al., 2012), for mineral and rubber modified polypropylene in (Delhaye et al., 2010) and semi-crystalline polyamide 66 in (Maurel-Pantel et al., 2015) within the Iosipescu shear-test configuration.

In view of constitutive modeling, there have been research-efforts to obtain the material behavior under mechanical loads, see, for instance, (Haupt, 2002; Haupt and Sedlan, 2001) for elastomers or (Hartmann, 2006) for the case of a polymer. First, rate-dependence of the processes is of basic interest. Secondly, multi-step relaxation processes are used to estimate the internal equilibrium stress state of the material.

In the following, we present an experimental campaign in which the stress-stretch (strain) behavior of localized specimens is deduced from DIC-information. The experimental process pattern and loading paths are seen by the authors in the context of constitutive modeling, where we do not provide a model in this presentation.

The article is structured as follows: First, we draw on tensile experiments to show the rate-dependence, the relaxation behavior and the temperature-dependence of this behavior. Afterwards, similar processes are carried out using the shear test to study the shear behavior of the material.

## 2 Tensile Experiments within the Large Deformation Range

In order to identify the rate-dependence and the material equilibrium stress of the PP/PE copolymer thermo-plastic and the influence of the temperature on the mechanical characteristics, we performed monotonic isothermal uniaxial and multi-step tensile tests. All the tests were carried out in a universal testing machine equipped with a thermal chamber. The load was measured by means of a 10 kN load cell and the displacement field was measured by means of a digital image correlation system (GOM, 2011). The specimens were obtained from a thin foil (thickness 0.6 mm) and the contour was chosen according to (DIN EN ISO 527-3:2003-07, 2010)-type 5, see Fig. 1. The

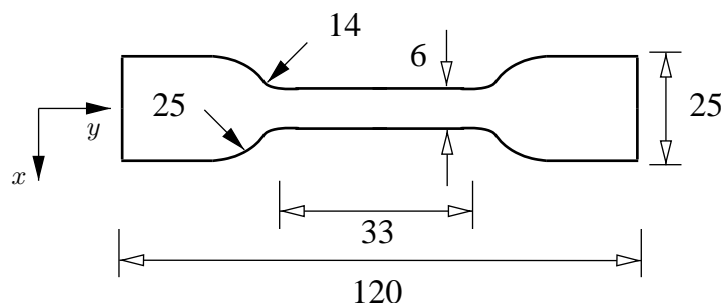


Figure 1: Geometry of the sample according to EN ISO 527-3 - measures in [mm] (thickness 0.6mm)

specimens were milled out of a stack of foils, taking care to consider the production in order to avoid influences of the production process. A random black and white pattern was applied on the surface of the specimens in view of the requirements of the DIC-system. The strain determination will be explained later in detail.

The rate-dependent effects are first investigated by means of uniaxial monotonic tensile tests performed at four different displacement-rates. Then, multi-step relaxation tests are applied to investigate the relaxation behav-

ior. The end-points of relaxation are assumed to define the initial equilibrium state of the material. These are used in overstress-type models to identify the equilibrium stress state, see, for example, (Liu and Krempl, 1979), (Haupt and Lion, 1995) and (Haupt and Sedlan, 2001). A first set of isothermal experiments is performed at a constant temperature  $\Theta = 20^\circ\text{C}$ . Afterwards, the influence of the temperature on the material behavior is also investigated by repeating the experiments at three temperatures, following the same process paths as those in the room-temperature case. Additionally, our investigation includes the compressibility (Poisson behavior) of the experiments (see Sect. 2.2 and Sect. 2.4), the loading-unloading behavior (see Sect. 3.2), the closeness of the experimental results (see Sect. B) and the anisotropy (see Sect. C).

## 2.1 Rate-dependence at Room Temperature

We start with isothermal monotonic tensile tests at a temperature  $\Theta = 20^\circ\text{C}$ , within the large deformation range and control the displacement-rates of the clamping of the testing device. Four different displacement-rates  $\dot{u}$ , varying between  $1\text{ mm s}^{-1}$  and  $10^{-3}\text{ mm s}^{-1}$ , are chosen according to a factor of ten with the purpose of investigating the rate-dependence of the material. Fig. 3 shows the prescribed displacement-time paths. The maximum displacement is defined so that strains of about 60 % are reached. Such a strain level corresponds to the ones occurring in the forming processes of sandwich composites. Under tension, the high level of strains induces necking phenomena (strain localization) within the PP/PE polymer specimens, see Fig. 1. The main drawback of localization phenomena is that the necking occurs at different places, sometimes also at two or three places - see, for a typical picture, Fig. 2. Thus, a classical strain-gage or a clip-on are not applicable. We chose a DIC-system to provide

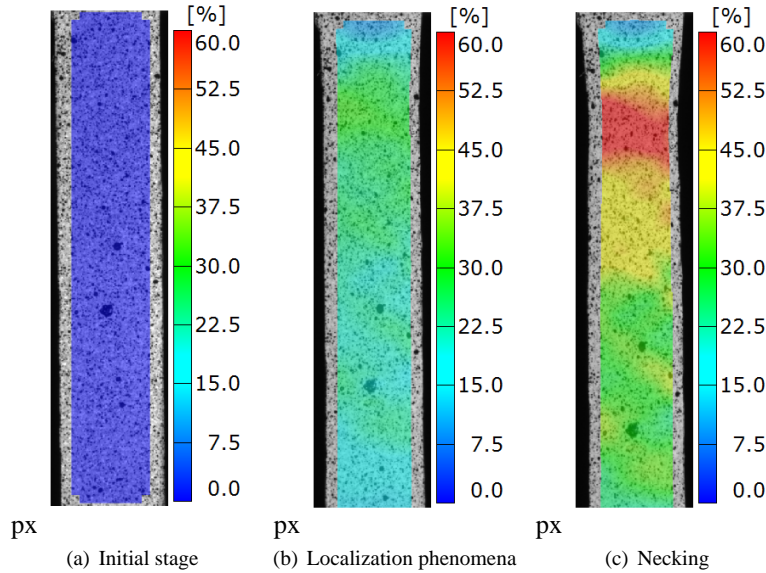


Figure 2: Axial technical strain field  $\varepsilon_{yy}^{(1)}$  during the evolution of the necking for an experiment at temperature  $\Theta = 20^\circ\text{C}$  measured by the DIC-system

the full-field displacement (and strains) information. After a test this data is evaluated and the place where the necking occurs is used for the strain information. In the localized area, we assume a homogeneous strain distribution laterally through the specimen. While this is applicable for most of the time span, there is a very short time-span in which it is not - which is when the localization starts spontaneously. In order to derive a constitutive equation, the corresponding stress state must be known too. Since the localized area is more or less perpendicular to the loading direction, the stresses are determined by the axial force divided by the initial cross-section  $A_q = 6 \times 0.6 = 3.6\text{ mm}^2$ . This type of stress, known in the Applied Sciences as engineering stress, is called 1st Piola-Kirchhoff stress in the Continuum Mechanics community. In view of the coordinate system in Fig. 1, we symbolize it by  $T_{Ryy}$ , where  $y$  defines the axial direction. Instead of using a strain-measure, we choose the notion of stretch (current length divided by original length), since it is independent of the choice of the strain measure. In A the calculation of the true stresses (Cauchy stresses) and possible strain measures are explained. Since a few decades, the yield behavior of polymers is an important point of discussion within the scientific community. In addition to reviewing the yield behavior of polymers, (Ward, 1971) and (Raghava et al., 1973) also discussed the theoretical aspects of extending the the yield criteria from the ductile metals to polymers, based on the available experimental data on polymers, as well as the need for a generally accepted yield criterion for this class of solids.

Further, (Bowden, 1973) and (Ward and Hadley, 1993) present criteria to define the yield point of polymers that do not clearly show an experimental maximum stress. The tensile experiments performed on the PP/PE copolymer show a clear peak stress, which is why our work refers to the definition of yield stress used, for example, in (Haward and Young, 1997) and (Zhou and Mallick, 2002), where the maximum stress value in the stress-stretch curve is suggested as the yield stress.

The investigation on the rate-dependence at room temperature – see Fig. 3 for the loading path – is presented

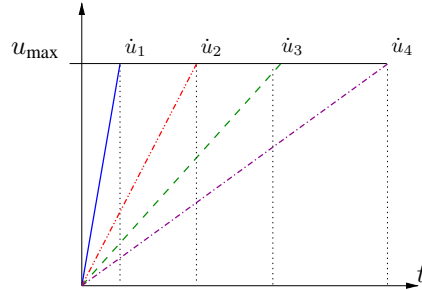
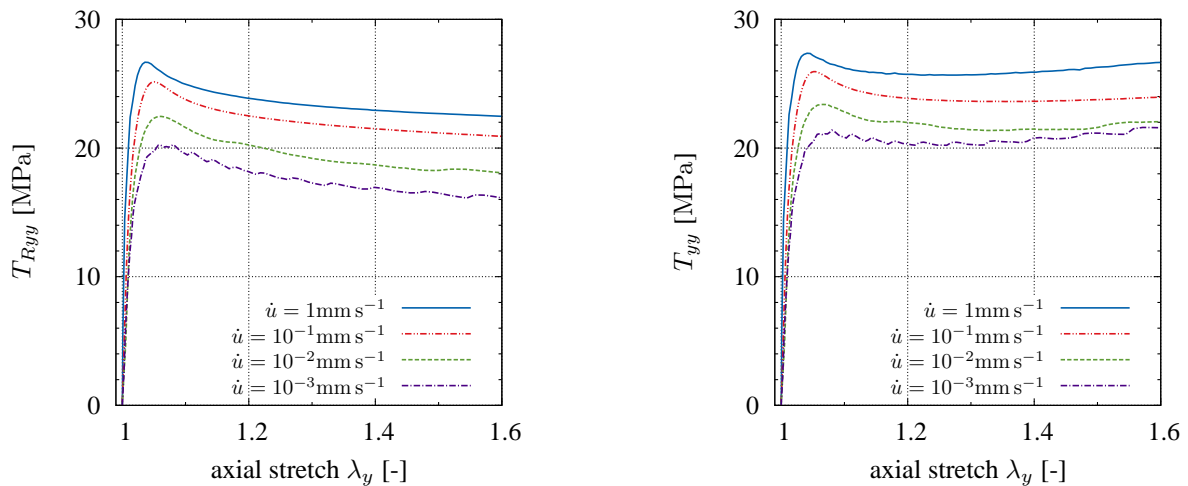


Figure 3: Prescribed loading path

in Fig. 4(a) in form of a comparison between the tests performed at the four displacement-rates. After reaching



(a) 1st Piola-Kirchhoff stress - stretch behavior

(b) Cauchy stress - stretch diagram

Figure 4: Stress-stretch behavior at different displacement-rates and  $\Theta = 20^\circ\text{C}$

the yield stress, the 1st Piola-Kirchhoff stress shows softening and the necking propagates through the specimen. Fig. 4(a) also shows a non-linear rate-dependence of the material, where a higher level of stress corresponds to a higher displacement-rate. During the experiments the lateral stretch  $\lambda_x$  in the width direction of the specimen is also measured by means of the DIC-system. Moreover, this provides the possibility to determine the component of the Cauchy stress,  $T_{yy}$ . The component of the Cauchy stress  $T_{yy}$  (called true stress) is represented in Fig. 4(b) with respect to the axial stretch  $\lambda_y$ . Again, the non-linear dependence of the Cauchy stresses on the displacement-rate can be observed. Furthermore, the Cauchy stress is characterized by an initial slope followed by strain softening. A so-called strain hardening starts at a stretch level of around  $\lambda_y \approx 1.4$ . The information on the stretch-rate, computed within the necking area, is finally reported in Fig. 5. In the necking area, it clearly shows non-linear behavior - although the applied load is increased linearly. As it is not possible to predict where exactly the localization phenomena will take place within the specimen, the evaluation process takes place after the test, by means of the DIC-system. This is a more time-consuming procedure than the classical tensile test evaluation. Each “digital image project” has to be studied to find the localization region, which has to be evaluated in view of the axial and lateral stretch.

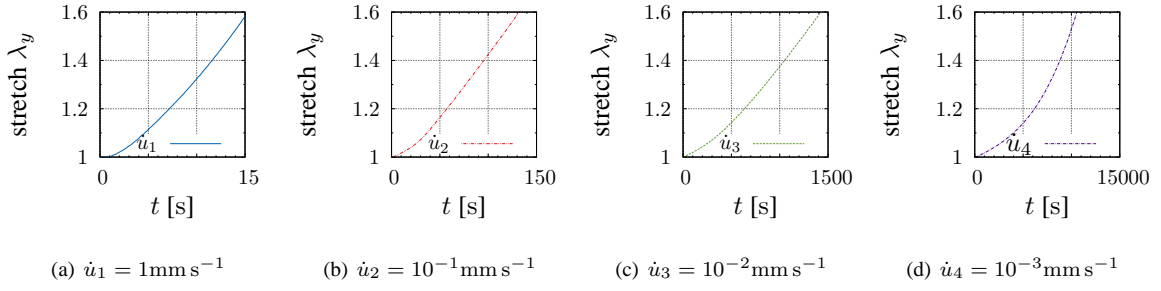
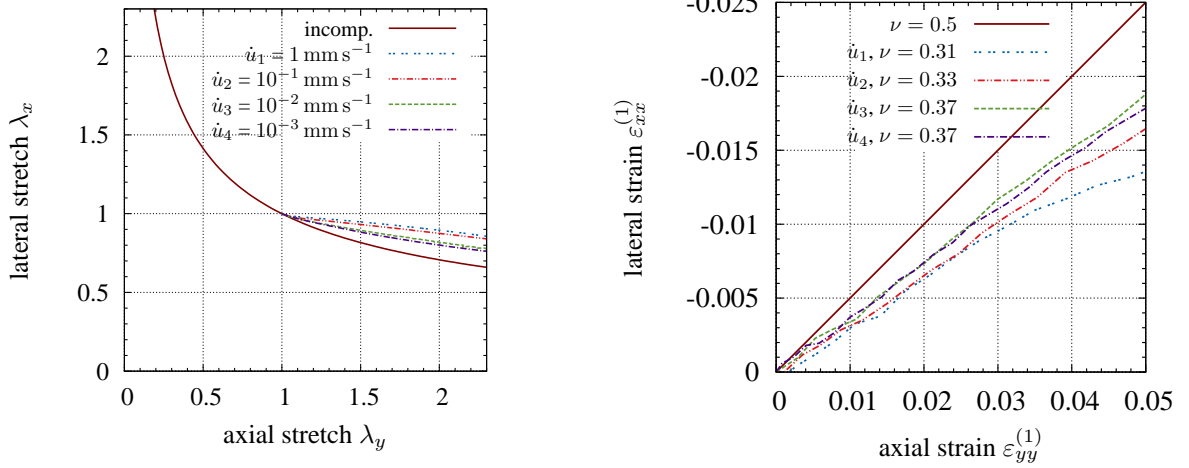


Figure 5: Axial stretch-time diagrams

## 2.2 Investigation on Compressibility

The compressibility of PP/PE is discussed by considering the isothermal tensile experiments presented in Subsection 2.1. In A the mathematical relations of the volumetric deformations are provided. Fig. 6(a) shows the lateral



(a) Lateral stretch behavior at different displacement-rates

(b) Transverse strain  $\varepsilon_{xx}^{(1)}$  versus axial strain  $\varepsilon_{yy}^{(1)}$  (engineering strains)

Figure 6: Investigation on compressibility

stretch  $\lambda_x$  versus the axial stretch  $\lambda_y$  measured for the tensile tests performed at different rates and compared to the theoretical case of incompressibility  $\det \mathbf{F} = \lambda_y \lambda_x^2 = 1$ , i.e.  $\lambda_x = \lambda_y^{-1/2}$ . Here, we assume  $\lambda_z = \lambda_x$ . In the tensile range the lateral stretches  $\lambda_x$  decrease at larger axial stretch-rates. The experimental tensile tests on the PP/PE polymer blend show that the assumption of incompressibility is not justified.

A further study is done within the small deformation range, for the same set of experiments. Fig. 6(b) shows the lateral strain  $\varepsilon_{xx}^{(1)}$  versus the axial strain,  $\varepsilon_{yy}^{(1)}$ , in the direction of the tensile load (see A for the strain and stretch definition). The values of the Poisson ratio  $\nu$  of the experiments are calculated by means of  $\varepsilon_{xx}^{(1)} = -\nu \varepsilon_{yy}^{(1)}$ , making use of a linear least-square method. The diagram shows that the values of Poisson ratio  $\nu$  increase with the decrease of the strain-rate, differing from the incompressibility value  $\nu = 0.5$ . The results are in agreement with the scientific literature on polymer blends, see (G'Sell and Jonas, 1979), (G'Sell et al., 2004) and (Petronyuk et al., 2002), where the Poisson ratio of PP/PE blends and their single components, evaluated according to different experimental analyses within the small deformation range, lie in a range of 0.37 – 0.41.

## 2.3 Relaxation Behavior

### 2.3.1 Long-time Relaxation Test

According to (Haupt, 2002), (Haupt and Lion, 1995) and (Haupt and Sedlan, 2001), we assume that a material has an internal equilibrium state, at which no further time-dependent changes occur. Since infinite slow loading processes are not possible, multi-step relaxation tests are used - assuming that the termination points of relaxation will approximately determine, the equilibrium stress state. In order to estimate the holding times, a long-time relaxation process is performed. For the whole test, we choose a total holding time of 26 hours. The value of the maximum displacement guarantees the desired level of strains within the large deformation range. The test has a displacement-rate  $\dot{u} = 10^{-2} \text{mm s}^{-1}$  during the loading phase. The prescribed path of the long-time relaxation test is illustrated by Fig. 7(a) together with the axial stretch  $\lambda_y$ , within the first three hours of the test, - where it is

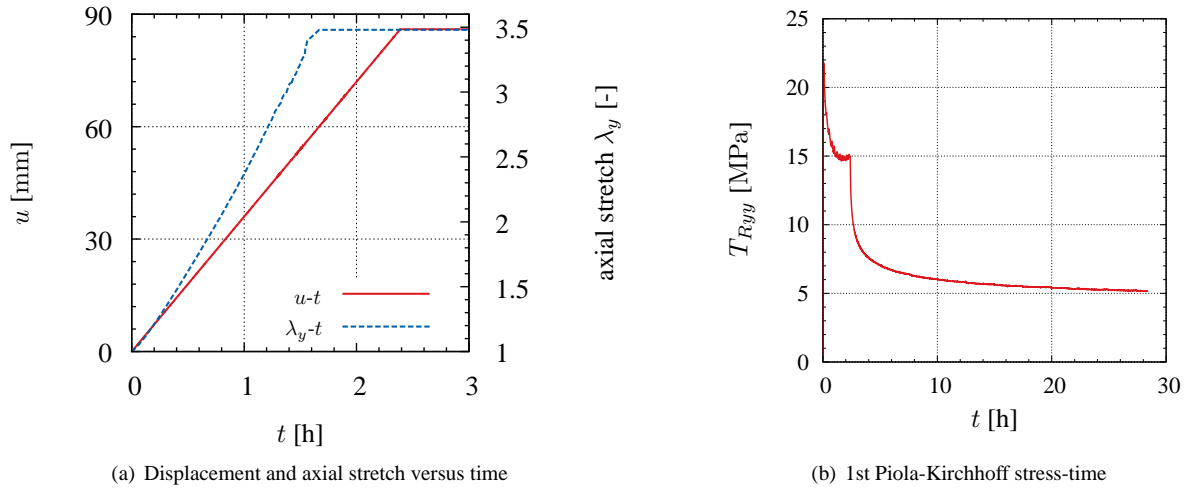


Figure 7: Long-time relaxation process

shown how a linear displacement path is associated to a non-linear development of the axial stretch  $\lambda_y$ . Only the first 3 hours are considered in the figure. In Fig. 7(b) the stress  $T_{Ryy}$  is depicted with respect to the time, showing a first decrease in the values due to the evolution of necking and a second decrease due to the relaxation process. After 26 hours the relaxation process is not yet finished. For PP/PE foil specimens, it is not possible to arrange for a relaxation path - in which the load is increased to its maximum and then re-loaded after each hold-time in order to reach the saturation value faster (horizontal slope) - which is due to buckling in the unloading phase, see, (Sedlan, 2000) or (Haupt and Sedlan, 2001) in regard of this process.

### 2.3.2 Multi-step Relaxation Tests within the Large Deformation Range

The multi-step relaxation process is investigated within the large deformation range. Afterwards, the equilibrium stress curve will be obtained from estimated termination points of relaxation for material modeling purposes. Here, the investigation of the large deformation range is presented for the multi-step relaxation test. Within this range, two different prescribed loading-unloading paths are chosen to characterize the behavior of the material. According to the experience of the long-time relaxation process in Fig. 7(b), we chose a hold-time of five hours so that the overall time is not too long. Fig. 8(a) shows the prescribed displacement-time path of the two tests, where the same value of maximum displacement is reached and a hold time of five hours is chosen for each step. The first multi-step test consists of five loading and two unloading steps while the second multi-step test has one loading step followed by five unloading steps. Fig. 8(b) shows the relaxation behavior of the 1. Piola-Kirchhoff stress  $T_{Ryy}$  during the time. The results of the tests are presented in Figs. 9, where a pronounced relaxation dominates the material behavior. Figs. 10 show the termination points of relaxation together with the monotonous loading paths, where we take only the first four termination points of the process in Fig. 8(a) in order to obtain a basic impression of constitutive modeling.

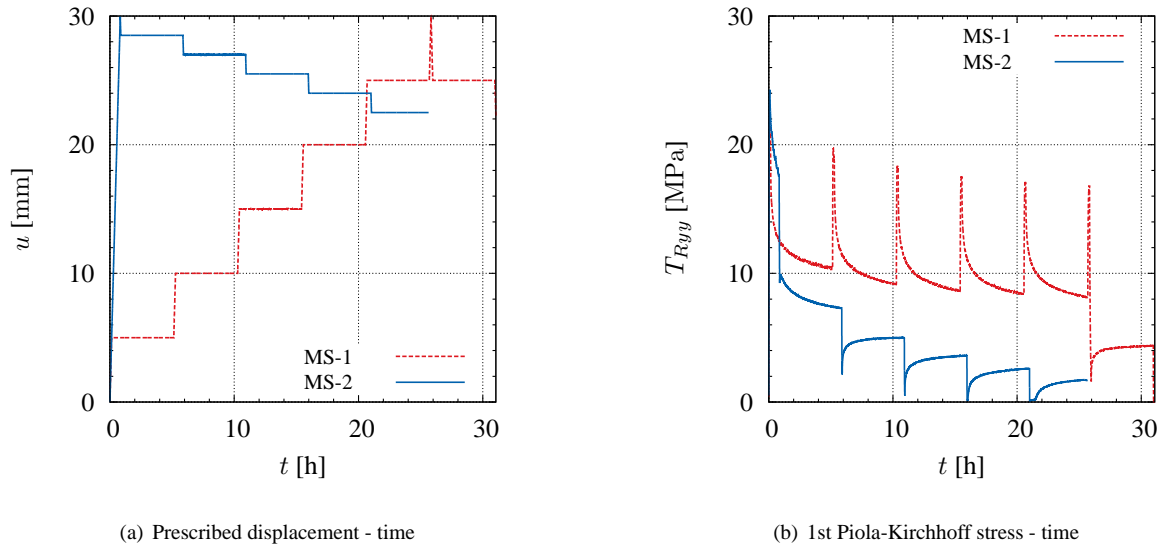


Figure 8: Multi-step relaxation tests within the large deformation range

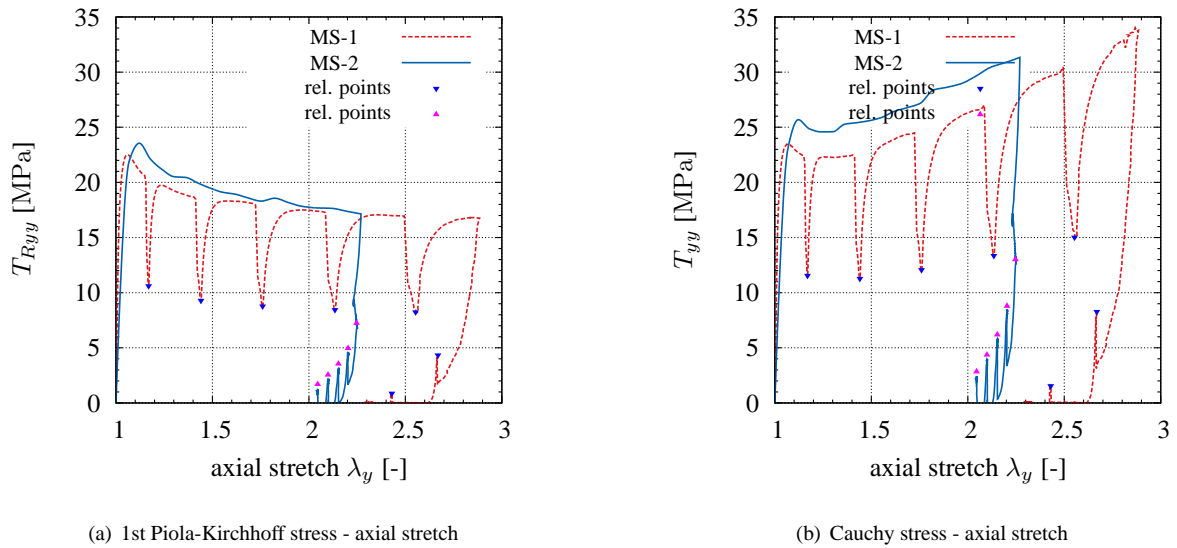


Figure 9: Multi-step relaxation behavior within the large deformation range

## 2.4 Temperature-dependence in Tensile Tests

In order to investigate the temperature-dependence of the thermo-plastic PP/PE copolymer, we employ specimens with the same geometrical characteristics as used for the experiments at  $\Theta = 20^\circ\text{C}$  and also the same experimental set-up. The glass transition temperature  $\Theta_g$  of  $-12^\circ\text{C}$  and the melting temperature  $\Theta_m$  of  $160^\circ\text{C}$  are estimated in advance by means of Temperature-Modulated Differential Scanning Calorimetry Analysis (TMDSC) and Dynamic Mechanical Analysis (DMA) on the PP/PE foil specimens, according to the methodologies described in (Ehrenstein et al., 2004) (see Sect. D).

Three additional temperatures are chosen in the range between the glass transition temperature  $\Theta_g$  and the melting temperature  $\Theta_m$  so as to repeat the isothermal tensile tests at the same displacement-rates as the tests at  $\Theta = 20^\circ\text{C}$ . The investigated temperatures are  $\Theta = -10^\circ\text{C}$ ,  $50^\circ\text{C}$ ,  $120^\circ\text{C}$ . Particularly, the temperature  $\Theta = 120^\circ\text{C}$  characterizes the production temperature of the sandwich composite, see (Palkowski et al., 2013).

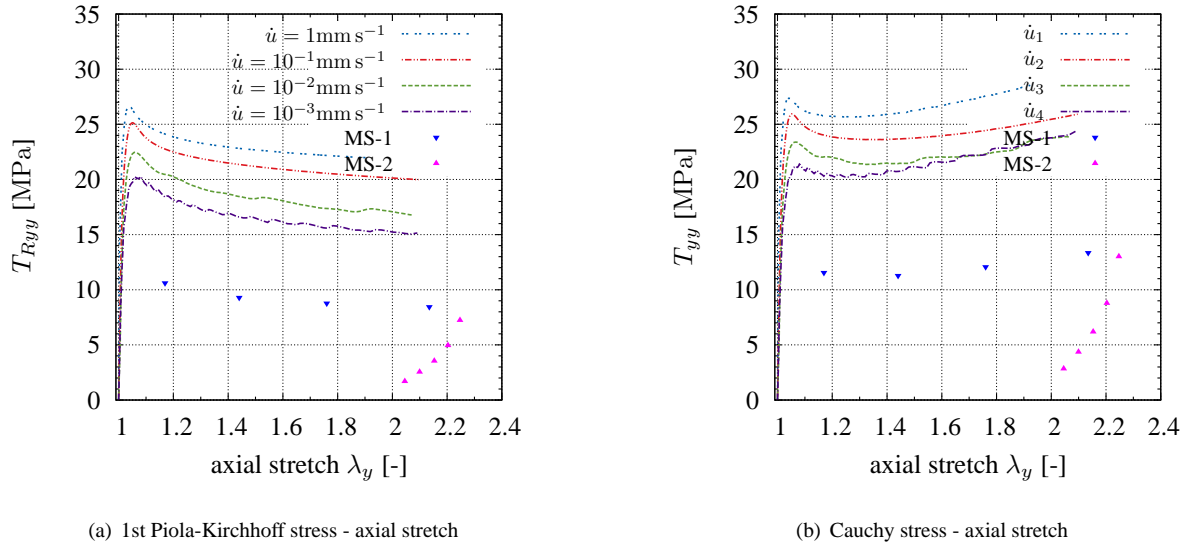


Figure 10: Comparison between monotonic tensile tests and termination points of multi-step tests within the large deformation range

Multi-step relaxation tests are performed, following the same loading-unloading path for each chosen temperature. The evolution of the 1st Piola-Kirchhoff stress during the time is shown too, see Figs. 11 - 13. Based on the

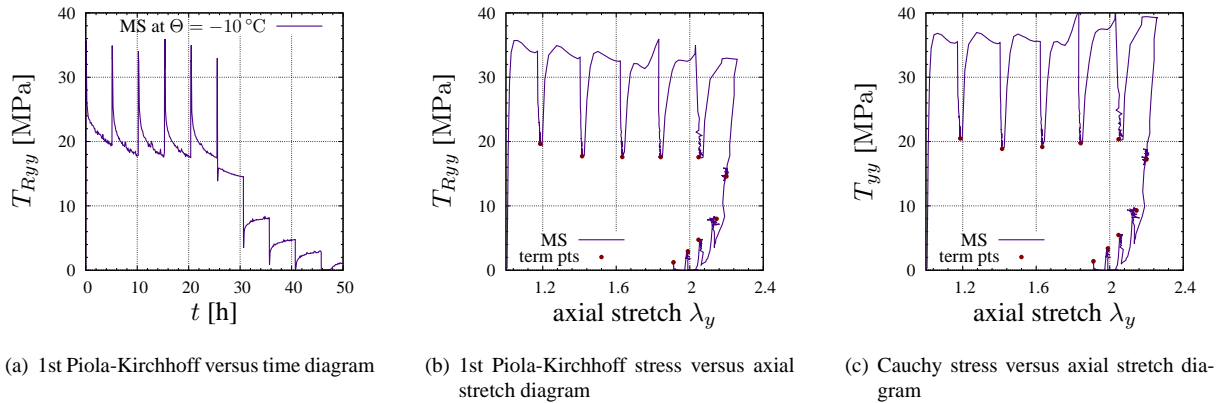


Figure 11: Multi-step test at  $\Theta = -10^\circ\text{C}$

analysis of the stress-stretch behavior of these figures, Fig. 11, Fig. 12 and Fig. 13, it is possible to determine the influence of the temperature on the level of stress. By assuming the same loading-unloading path, displacement-rate and holding time, the total amount of stresses decreases with the increase of temperature. As previously observed for the multi-step relaxation test at room-temperature, the end-points of relaxation describe an equilibrium curve which lies below the test performed at the slowest displacement-rate. In particular, the measured amount of relaxation is not the same for all the multi-step tests - and they decrease with the increase of temperature. Figs. 11 - 13 illustrate the temperature-dependence of the multi-step test: For each temperature, the end-points delineate an equilibrium curve, that, with increasing temperature, approaches the slowest displacement-rate test. A further analysis of the isothermal monotonic uniaxial tests highlights the non-linear rate-dependence, characterizing the tests at all the investigated temperatures. Again, we assume the prescribed displacement paths of Fig. 3. In Figs. 14 -to 16 the monotonous tensile tests are shown for varying temperatures ( $\Theta = -10^\circ, 50^\circ, 120^\circ$ ), once again indicating the pronounced rate-dependence and the strong influence on the temperature. Fig. 17(a) reports the behavior of PP/PE in terms of 1st Piola-Kirchhoff stress - axial stretch diagram. For all of the investigated temperatures, the copolymer exhibits an initially stiff slope followed by yielding. After that, the stress-stretch behavior is characterized by strain softening, which corresponds to the initiation of the macroscopic phenomenon of necking. With the increase of temperature, the material's response is characterized by a lower total amount of

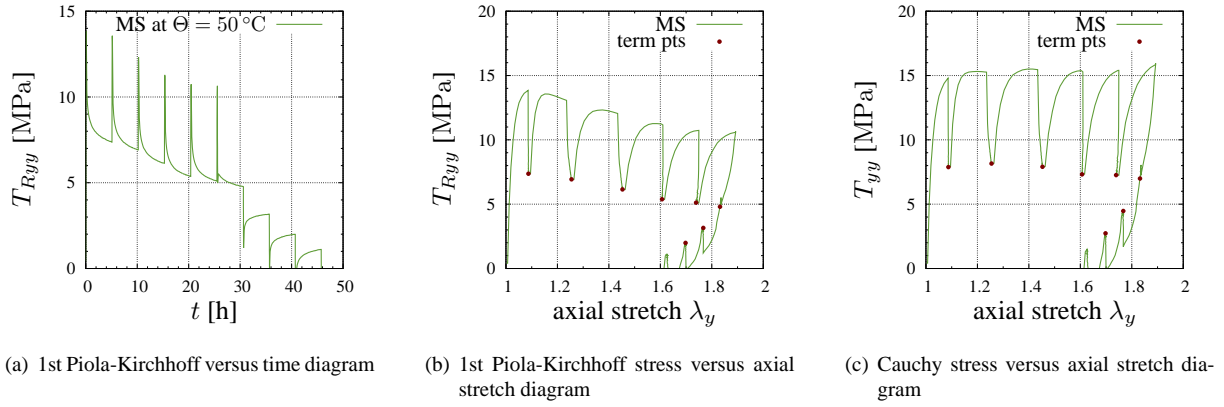


Figure 12: Multi-step test at  $\Theta = 50\text{ }^{\circ}\text{C}$

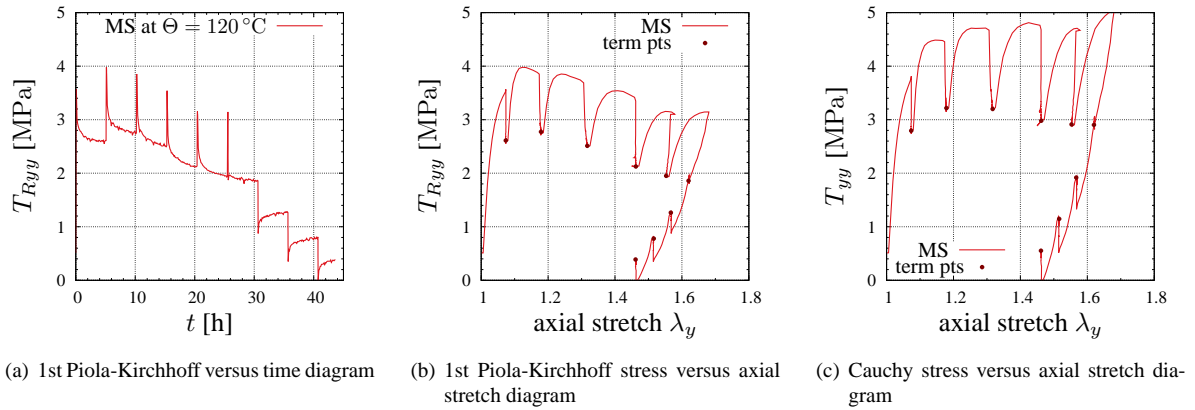


Figure 13: Multi-step test at  $\Theta = 120\text{ }^{\circ}\text{C}$

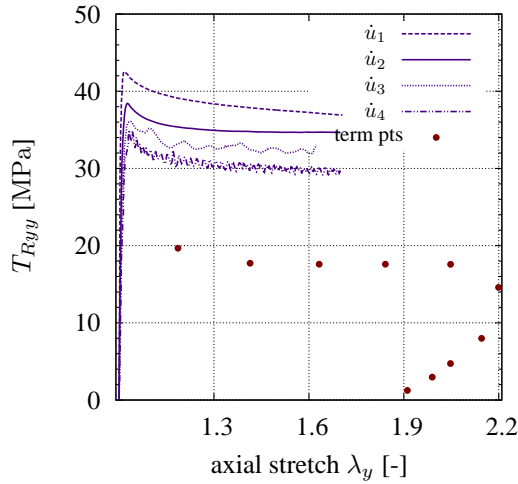
stress. Finally, Fig. 17(b) shows the Cauchy stress - axial stretch diagram. As previously shown for other kinds of polymers (Arruda et al., 1995), the material exhibits strain softening followed by strain hardening after the yield stress. Furthermore, for the PP/PE copolymers, the hardening is more pronounced at higher temperatures.

Finally, the study of the influence of the temperature on the Poisson ratio is reported. Fig. 18(a) and Fig. 18(b) illustrate the tests performed at the fastest and the slowest displacement-rates in terms of (engineering) transverse strain  $\varepsilon_{xx}^{(1)}$  versus axial strain  $\varepsilon_{yy}^{(1)}$ . In agreement with the results on polymers, see (Drozdov, 1998), (Pandini and Pegoretti, 2011), and (Haward and Young, 1997), the Poisson ratio increases with the increase of temperature and decreases with the displacement-rate of the experiments.

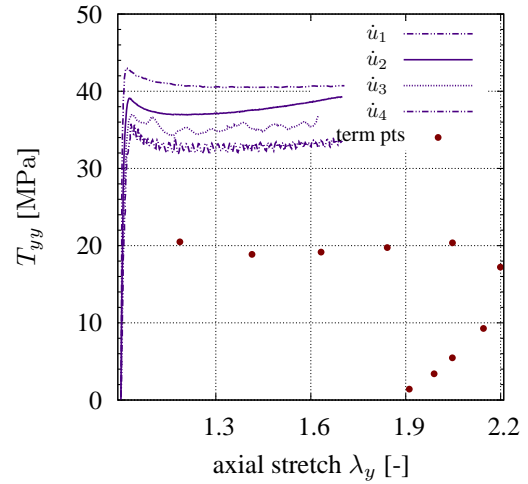
The temperature also has considerable influence on the development of the necking within the PP/PE specimens: during the experiments performed at different temperatures a more homogeneous distribution of the strain was observed with the increase of the temperature, both within and out of the region of localization, as it is shown in Fig. 19, where the strain field of a specimen tested at  $\Theta = 50\text{ }^{\circ}\text{C}$  is reported.

### 3 Investigation within the Small Deformation Range

Apart from the large strain case, the experimental behavior of the material is studied within the small deformation range, i.e. close to the yield point and the macroscopic localization. This is done in order to gain more detailed insight into the equilibrium stress behavior which is necessary in the scope of material modeling. In the following, we present a comparison between the monotonic tensile tests and the multi-step relaxation test, which are performed at constant strain-rate. In this range of deformation, the material does not show the macroscopic phenomena of necking, so the DIC-system is not used. The experiments are monitored by means of a non-contact, high-resolution video extensometer provided by Zwick-Roell, which recognizes the gauge marks on the specimen

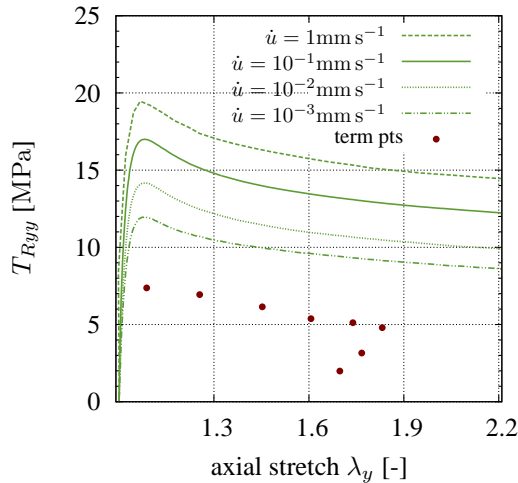


(a) 1st Piola-Kirchhoff stress-axial stretch

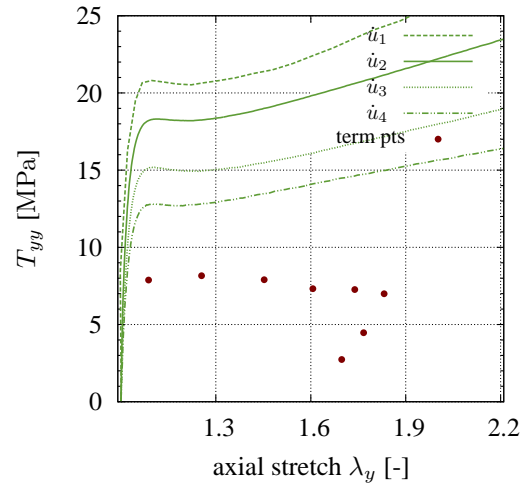


(b) Cauchy stress-axial stretch

Figure 14: Tests at  $\Theta = -10^\circ\text{C}$ : comparison between monotonic isothermal tensile tests at four different displacement-rates and multi-step test (displacement rate:  $\dot{u}_1 = 1\text{mm s}^{-1}$ ,  $\dot{u}_2 = 10^{-1}\text{mm s}^{-1}$ ,  $\dot{u}_3 = 10^{-2}\text{mm s}^{-1}$ ,  $\dot{u}_4 = 10^{-3}\text{mm s}^{-1}$ )



(a) 1st Piola-Kirchhoff stress-axial stretch



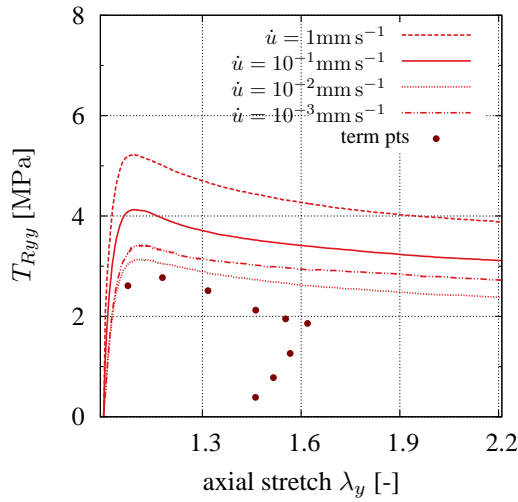
(b) Cauchy stress-axial stretch

Figure 15: Tests at  $\Theta = 50^\circ\text{C}$ : comparison between monotonic isothermal tensile tests at four different displacement-rates and multi-step test

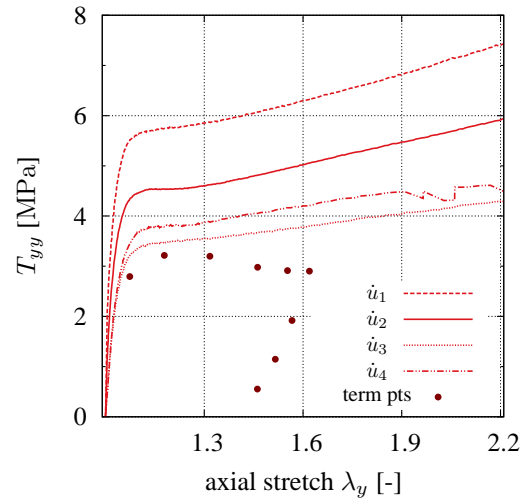
surface and converts them into extensions. Furthermore, a second displacement-controlled multi-step relaxation test is performed and monitored by means of the DIC-system and then compared, within the small deformation range, to the displacement-controlled tensile experiments, previously presented in Sec. 2. Finally, the loading-unloading behavior of the material is studied experimentally too, in order to quantify the remaining deformations. The entire investigation within the small deformation range is carried out at a constant temperature  $\Theta = 20^\circ\text{C}$ .

### 3.1 Monotonic and Multi-step Tensile Tests

The rate-dependence of the PP/PE material is investigated within the small deformation range by means of monotonic strain-controlled tests, performed at four different strain-rates, going from  $\dot{\epsilon} = 2 \times 10^{-2}\text{s}^{-1}$  to  $\dot{\epsilon} = 2 \times 10^{-5}\text{s}^{-1}$ , decreasing according to a factor of ten, and by means of a multi-step relaxation test performed

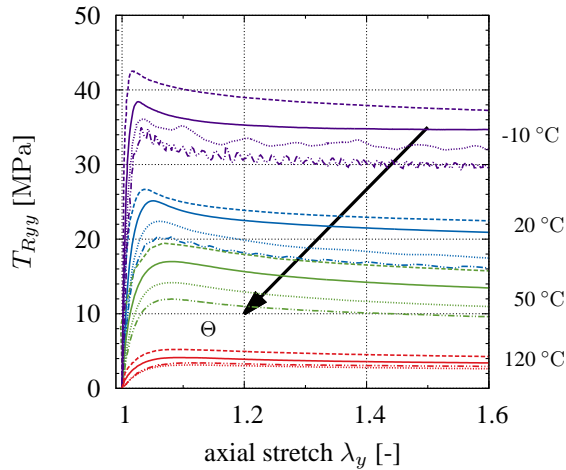


(a) 1st Piola-Kirchhoff stress-axial stretch

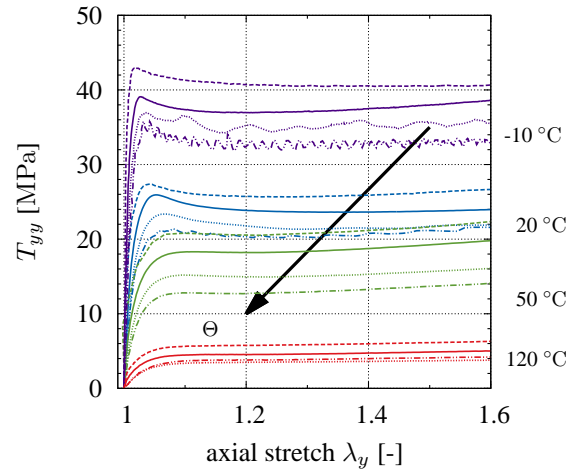


(b) Cauchy stress-axial stretch

Figure 16: Tests at  $\Theta = 120^\circ\text{C}$ : comparison between monotonic isothermal tensile tests at four different displacement-rates and multi-step test



(a) 1st Piola-Kirchhoff stress-axial stretch



(b) Cauchy stress-axial stretch

Figure 17: Comparison among monotonic isothermal tensile tests at four different temperatures and displacement-rates (the arrows indicate the experiments for increasing temperature)

at the slowest strain-rate. The multi-step relaxation test is presented first. Fig. 20(a) shows the prescribed strain-time path: The maximum value of the technical axial strain  $\varepsilon_{\max} = 4\%$  is reached by means of five loading steps and two unloading steps, all characterized by a holding time of 5 hours. Fig. 20(b) reports the axial engineering stresses  $T_{Ryy}$  with respect to the axial strain  $\varepsilon_{yy}$ . The termination points of relaxation are highlighted.

The monotonic strain-controlled tests are performed, according to the prescribed path of Fig. 21(a), where the maximum strain  $\varepsilon_{\max} = 4\%$  is reached and the unloading branch of the path stops when the forces reach the zero value. The comparison between the monotonic tests and the multi-step relaxation test is shown in Fig. 21(b) in terms of stress-strain diagrams. As a result of the comparison between the experiments a strong rate-dependence can be observed for the copolymer. The stresses increase with the increasing strain-rate, and the end-points of relaxation indicate an equilibrium hysteresis that lies below the slowest strain-rate of the performed tests. Since remaining deformations can be observed also within the small deformation range, a further investigation is addressed in Sec. 3.2.

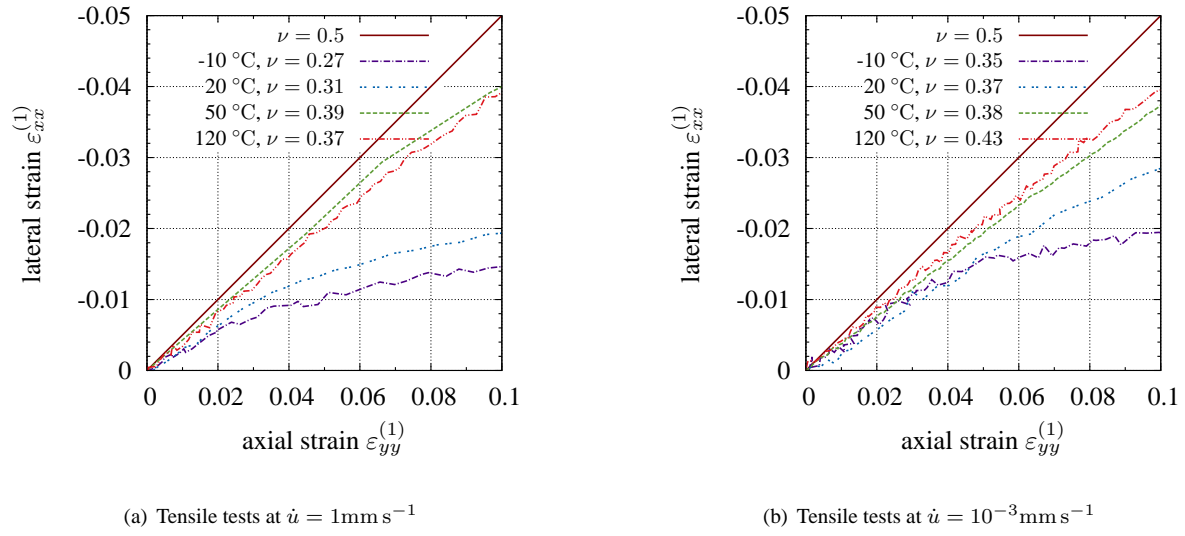


Figure 18: Transverse strain  $\varepsilon_{xx}^{(1)}$  versus axial strain  $\varepsilon_{yy}^{(1)}$  (engineering strains) at different temperatures and displacement rates

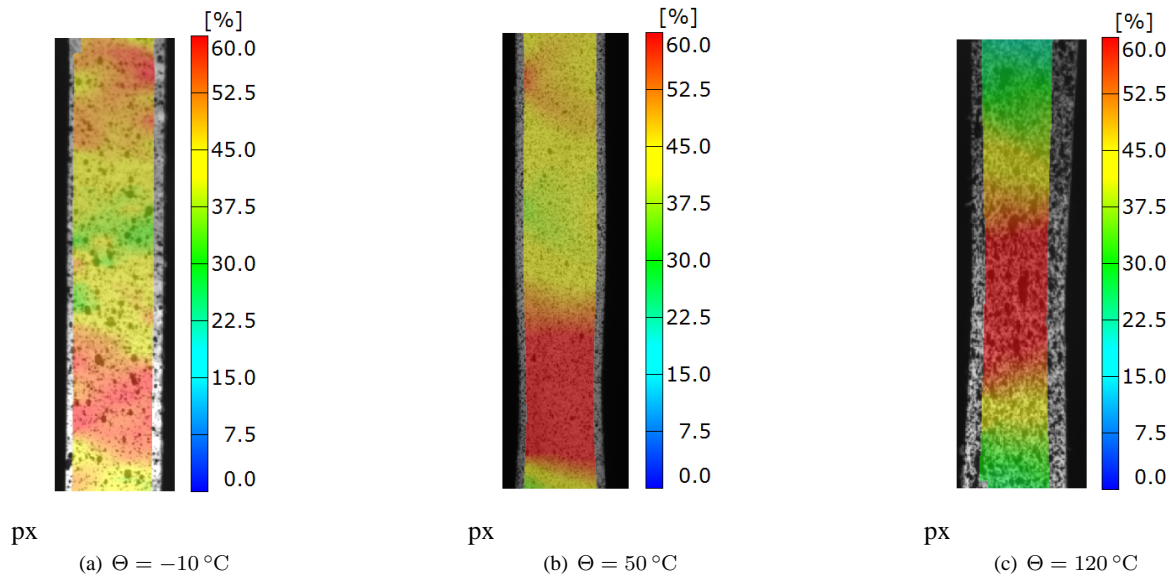


Figure 19: Axial technical strain field  $\varepsilon_{yy}$  during the evolution of the necking for experiments at a displacement-rate  $\dot{u} = 10^{-1} \text{ mm s}^{-1}$  and different temperatures measured by the DIC-system

### 3.2 Loading-unloading Behavior

The loading-unloading behavior within the small deformation range is investigated by means of a displacement controlled test, the prescribed path of which consists of a loading branch up to a maximum value of the displacement  $u_{\max} = 0.1 \text{ mm}$  and an unloading branch. It reaches a value of the displacement corresponding to a force of almost zero and is kept constant for 5 hours, as it reported in Fig. 22(a). The test is performed at the slowest displacement-rate  $\dot{u} = 10^{-3} \text{ mm s}^{-1}$ .

The stress versus stretch behavior of the PP/PE polymer blend material is shown in Fig. 22(b). The relation between the axial component of both the 1st Piola-Kirchhoff stress  $T_{Ryy}$  and Cauchy stress  $T_{yy}$  with respect to the axial stretch  $\lambda_y$  is non-linear. Furthermore, when the stress vanishes at the unloading step, the material shows residual deformations, which remain also after the holding period of 5 hours. The results of this test are in agreement

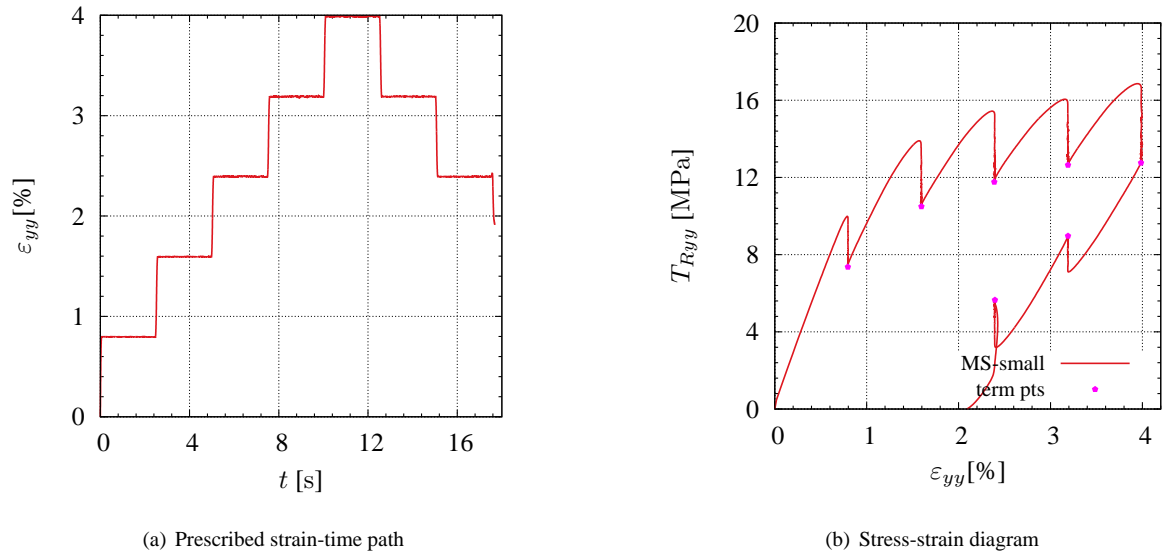


Figure 20: Multi-step relaxation test within the small deformation range

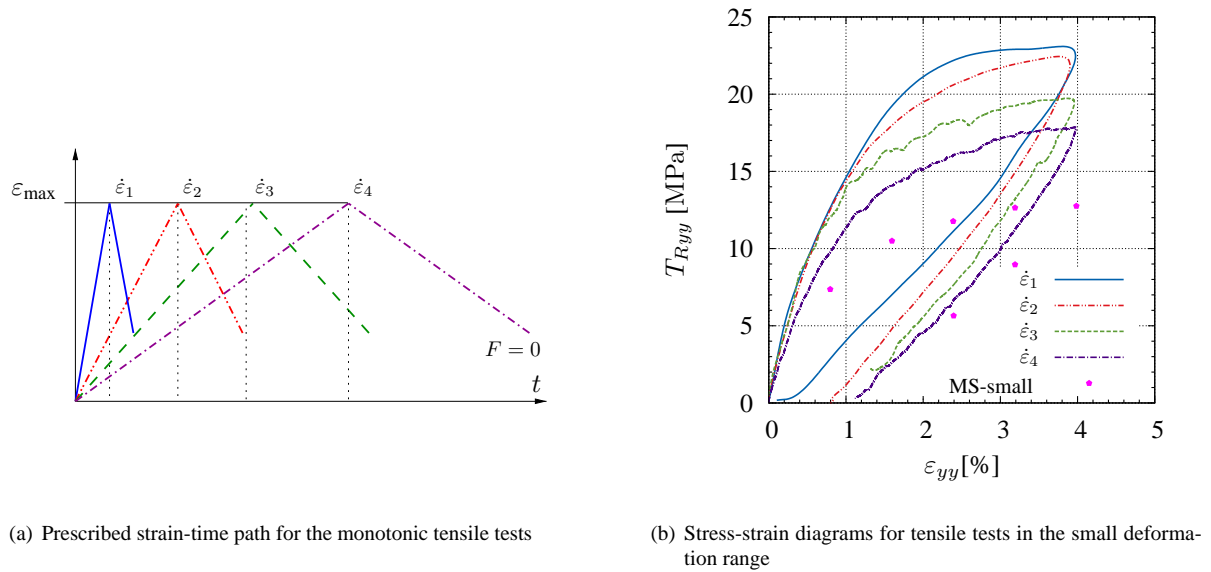


Figure 21: Comparison between the monotonic tensile tests and the termination points of the multi-step test for the tensile experiments within the small deformation range ( $\dot{\epsilon}_1 = 2 \times 10^{-2} \text{s}^{-1}$ ,  $\dot{\epsilon}_2 = 2 \times 10^{-3} \text{s}^{-1}$ ,  $\dot{\epsilon}_3 = 2 \times 10^{-4} \text{s}^{-1}$ ,  $\dot{\epsilon}_4 = 2 \times 10^{-5} \text{s}^{-1}$ )

with (Drozdov and Christiansen, 2007) and (Drozdov, 2009), who performed cyclic tests on dumbbell-shaped specimens of high-density polyethylene and polypropylene within the small deformation range with a prescribed loading displacement-controlled and an unloading force-controlled path. In the mentioned study, at the end of the first cycle, the investigated thermo-plastics also show remaining deformations of comparable magnitude with the experiments on PP/PE shown in Fig. 23.

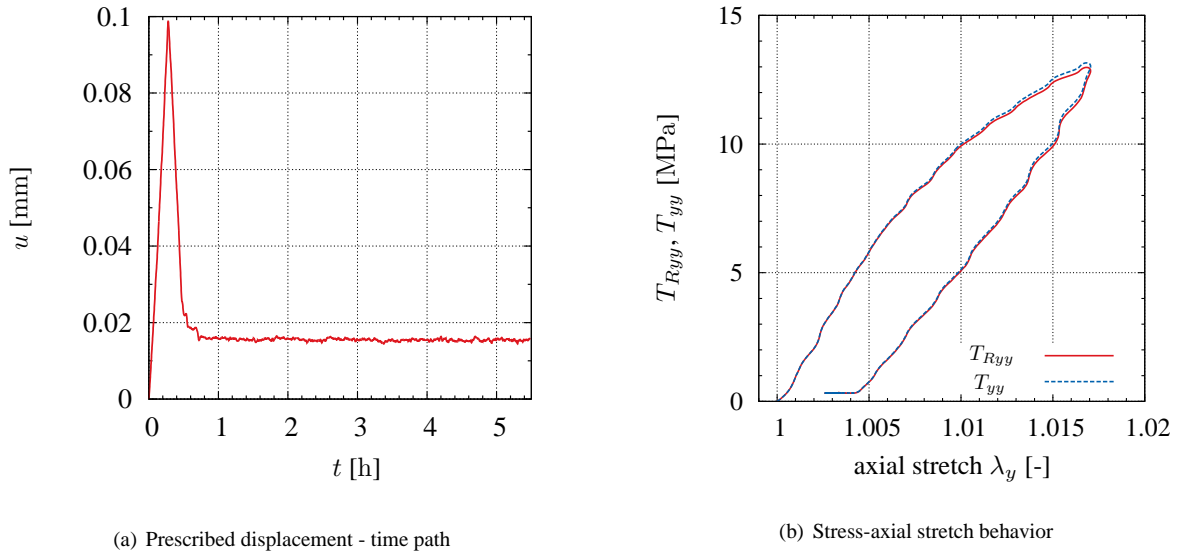


Figure 22: Loading-unloading behavior

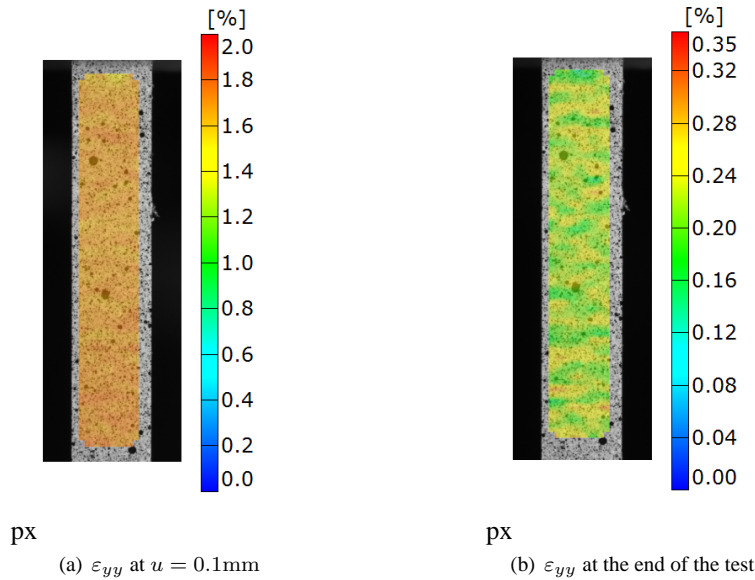


Figure 23: Strain field during the loading-unloading experiment: axial technical strain  $\varepsilon_{yy}$

## 4 Shear Experiments

### 4.1 Monotonic Shear Experiments

For a complete description of the material behavior, the in-plane shear properties of the PP/PE thermo-plastic are experimentally investigated. The PP/PE samples have a length  $l = 100\text{mm}$ , a height  $h = 78\text{mm}$  and a thickness  $t = 0.6\text{mm}$ . In order to perform shear tests on the copolymer foil specimens, the general mechanical principles of the three-rail shear test, see (ASTM D4255/D4255M-15a, 2015), are used for the design of a device able to generate an in-plane shear stress state, starting from the tensile load conditions of the existing testing machine (Sleuwen, 2014). Three main mechanical principles are considered in the development of the shear tool according to (G'Sell and Boni, 1983): the possible buckling if the specimen is not thick enough, the minimization of the normal stresses due to the grip of the clamping and the maximum load capacity of the machine. The load is applied to the external rails and transferred to the two symmetric areas of the specimen, while the central rail is fixed to the clamping of the testing machine. The relative displacement of the outer rails with respect to the central fixed

rail, induces a state of shear stress in the specimen, see Fig. 24. The thin flat specimen is fixed by means of three

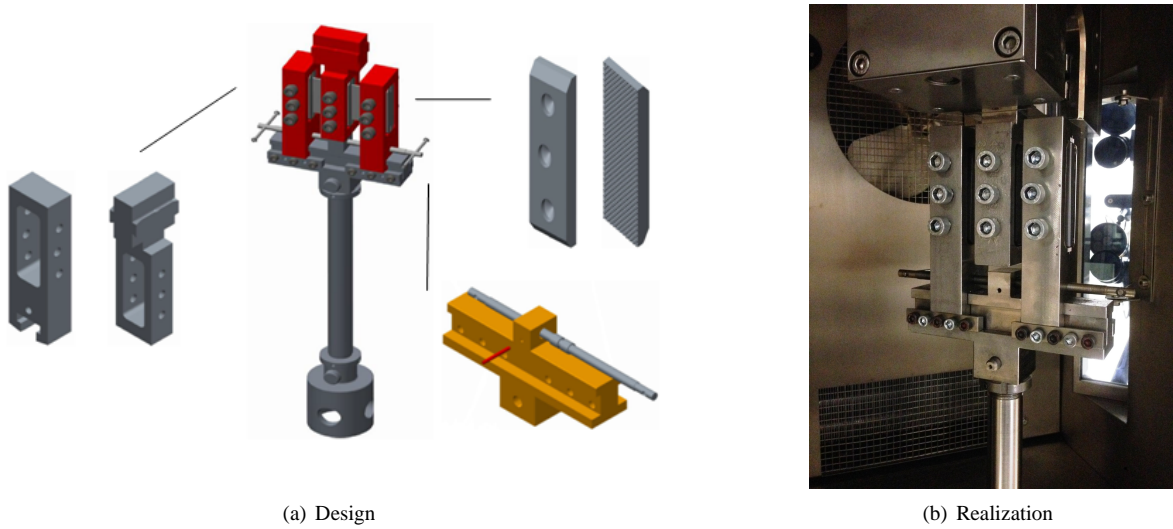


Figure 24: Shear device used for carrying out the experiments

couples of clamping, placed within the rails, that have rough inner surfaces and are held together by a total number of nine bolts. These are fastened by means of a torque wrench to ensure the desired fastening torque value of  $2.5 \text{ N mm}$ . There are no holes in the rectangular PP/PE foil specimens. The DIC-system is applied again in order to monitor the development of the strains within the two symmetric areas of the specimen. The displacement-rates and the temperatures investigated during the shear tests are the ones adopted for the monotonic tensile tests.

In this subsection the experiments at room temperature,  $\Theta = 20^\circ\text{C}$ , are presented. For all the performed tests, the shear stress  $\tau_{xy}$  of each area is derived from the vertical load  $F_y$  recorded during the experiments by means of  $\tau_{xy} = F_y / (2ht)$ . By considering the homogeneity of the strain distributions, excluding the small end areas of the specimen (which show edge effects, as will be discussed later on), the shear strain  $\gamma_{xy} = 2\varepsilon_{xy}$  is calculated for each time step. This is done as the average of the shear strains, in the middle of the shear zone, provided by the DIC-system.

The experimental investigation under shear conditions is carried out within the small deformation range. This choice is done because localization occurs and the shear stresses could not be assigned to the local shear strains in the large strain case under shear conditions. First, the repeatability of the shear tests is investigated by means of three experiments performed at a displacement-rate of  $\dot{u} = 10^{-1} \text{ mm s}^{-1}$ . The experiments are shown in Fig. 25(a), where the shear stress  $\tau_{xy}$  is plotted with respect to the shear strain  $\gamma_{xy}$ . Additionally, the mean value

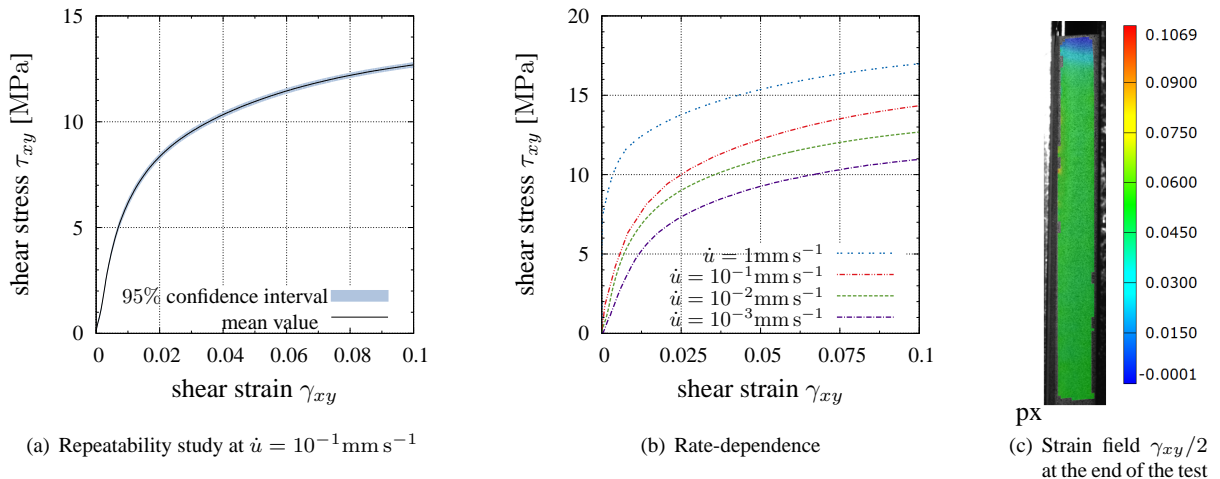


Figure 25: Shear tests at a temperature  $\Theta = 20^\circ\text{C}$  (3 tests)

of the tests and the corresponding standard deviation are determined. The standard deviation is about  $10^{-1}$  MPa, so that repeatability is assumed for the shear tests as well.

The rate-dependence of the shear tests is presented in Fig. 25(b), where the shear stress-strain response of the PP/PE is reported. Similarly to the tensile tests, the shear stress increases with the displacement-rate of the test, i.e. a pronounced non-linear rate-dependence is observable. The DIC-system serves to investigate the edge effects of the specimen's strain distribution. Such phenomena have already been considered in an early work of Whitney et al. (1971), who used the rail shear test to analytically study and experimentally investigate composite materials. Considering the theory of thin plates with two constrained edges and two free edges, the authors specifically suggest an aspect ratio of  $h/a \geq 10$ , between the height  $h$  and the width  $a$  of each free area of the specimen, in order to obtain a uniformly distributed state of shear without larger influence of the edge effects. For the underlying shear experiments, we choose an aspect ratio of  $h/a = 15.6$ . For the PP/PE copolymer, the experimental observation of the shear strain distribution provided by the DIC-system, see Fig. 25(c), only shows significant deviations in a small area of the free edges. Such localization phenomena cover a length of about the width of each symmetric area (i.e. 5 mm). The results are in agreement with a similar investigation on polyethylene by G'Sell and Boni (1983) and are considered to be negligible for the final evaluation of the shear strains.

## 4.2 Temperature-dependence of Shear Experiments

Here, we finally present the influence of the temperature on the shear behavior of the thermo-plastic copolymer. We repeated the shear experiments, keeping the same experimental set-up of the tests carried out at room temperature, and investigated the same displacement-rates and temperature fields. The DIC-system serves to study the shear strain field. The investigation is illustrated in the Fig. 26, where the response of the material to the temperature increase is shown by means of the shear stress  $\tau_{xy}$  versus the shear strain  $\gamma_{xy}$  relation for each considered rate. As in the case of tension, the shear stress of the PP/PE softens with the increase of temperature; nevertheless, the decrease of the shear stress with the increase of the temperature is slightly weaker than the stress decrease in the case of tension. Furthermore, the decrease of shear stress with the increase of the temperature is approximately the same for the fast as well as the slow displacements rates. In other words, the rate of the experiments does not have significant effect on the temperature-dependent decrease of shear stress. This is illustrated in Fig. 26, where for  $\gamma_{xy} = 0.08$ , the shear stress  $\tau_{xy}$  softens, when the temperature increases from  $\Theta = -10^\circ\text{C}$  to  $\Theta = 120^\circ\text{C}$ , for all the displacement rates.

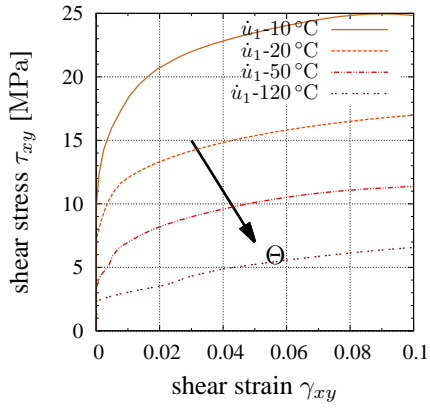
## 4.3 Multi-step Shear Experiments

The equilibrium curve of the shear experiments at different temperatures constitutes a further object of experimental investigation in the scope of material modeling. The multi-step relaxation shear tests are performed on the PP/PE specimens, within the small deformation range, at the slowest constant cross-head speed of  $10^{-2}\text{mm s}^{-1}$  and at the four considered temperatures  $\Theta = -10^\circ\text{C}, 20^\circ\text{C}, 50^\circ\text{C}$  and  $120^\circ\text{C}$ . Fig. 27(a) shows the prescribed displacement-time path assumed for all the investigated temperatures: Each step is described by a pre-defined value of the displacement that is kept constant for five hours, with a total number of five loading steps and five unloading steps to characterize the whole experiment.

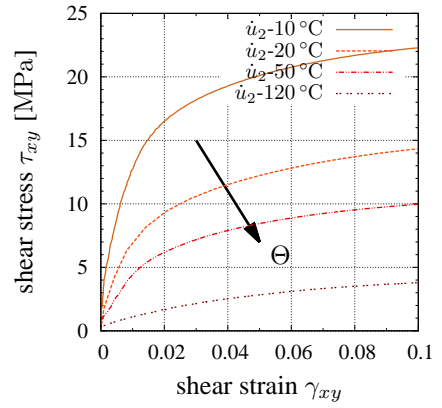
A comparison of the evolution of the stress over time is shown in Fig. 27(b). The relaxation behavior confirms the pronounced temperature-dependence also in the case of shear tests. Notably, the same retention time induces a relaxation in the PP/PE material that is smaller if the temperature increases. In addition, Fig. 28 shows the shear stress-shear strain diagrams. A comparison with the monotonic tests at each temperature suggests an equilibrium curve, with a loading and an unloading path, that is described by the termination points of the relaxation process and turns out less wide with an increase in temperature.

## 5 Conclusions

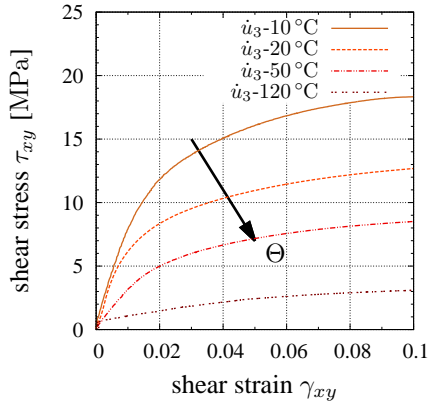
In this paper, we present the experimental study aiming to characterize how a thermo-plastic copolymer - which is used as core layer of sandwich metal/polymer/metal composite - responds to different prescribed rates and temperatures. Ultimately, the aim is to develop a material model that is able to take thermomechanical coupling effects into account.



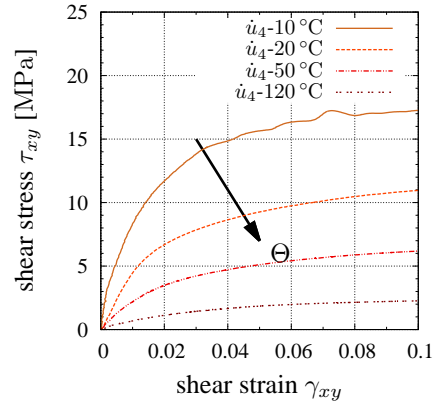
(a) Shear stress  $\tau_{xy}$  versus shear strain  $\gamma_{xy}$  of the tests performed at  $\dot{u}_1=1 \text{ mm s}^{-1}$



(b) Shear stress  $\tau_{xy}$  versus shear strain  $\gamma_{xy}$  of the tests performed at  $\dot{u}_2=10^{-1} \text{ mm s}^{-1}$

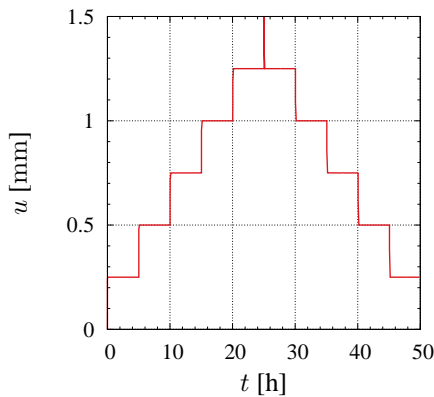


(c) Shear stress  $\tau_{xy}$  versus shear strain  $\gamma_{xy}$  of the tests performed at  $\dot{u}_3=10^{-2} \text{ mm s}^{-1}$

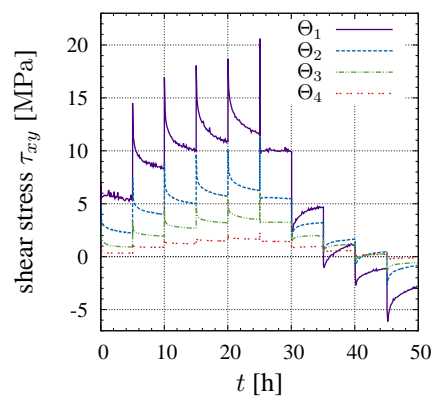


(d) Shear stress  $\tau_{xy}$  versus shear strain  $\gamma_{xy}$  of the tests performed at  $\dot{u}_4=10^{-3} \text{ mm s}^{-1}$

Figure 26: Temperature-dependence of the shear experiments at different displacement rates (the arrows indicate the experiments for increasing temperature)

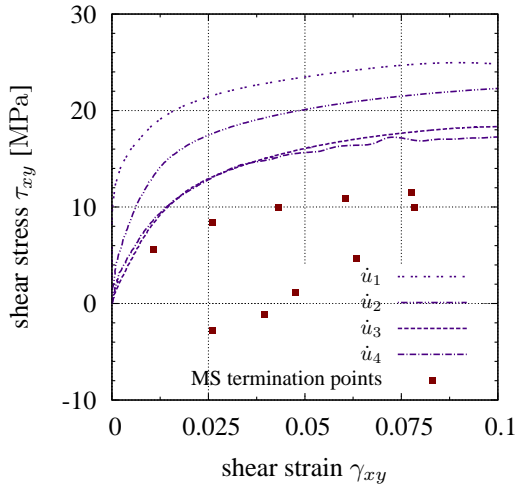


(a) Displacement-time path adopted for the multi-step shear tests at all temperatures

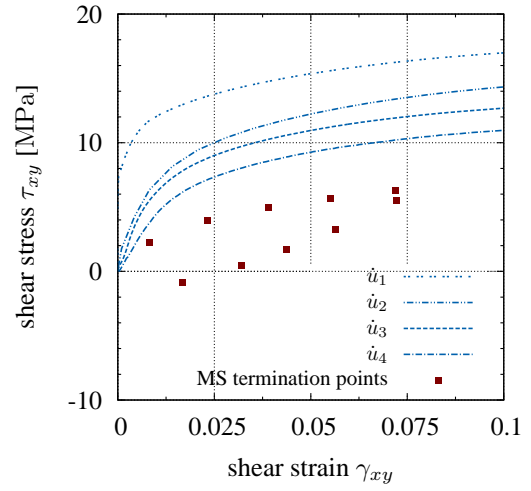


(b) Evolution of the shear stress  $\tau_{xy}$  during the time at different temperatures

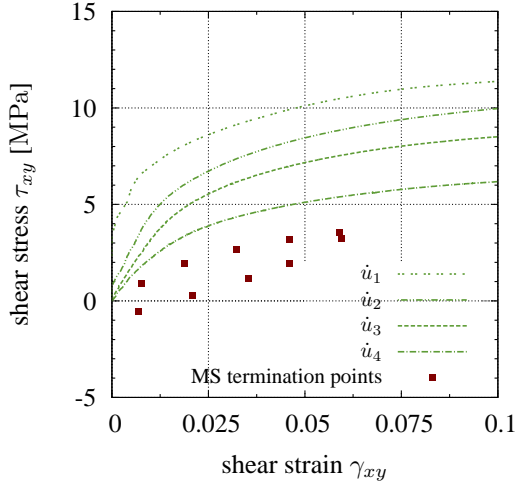
Figure 27: Multi-step shear tests: prescribed displacement path and stress-time behavior at temperatures  $\Theta = -10 \text{ }^\circ\text{C}$ ,  $\Theta = 20 \text{ }^\circ\text{C}$ ,  $\Theta = 50 \text{ }^\circ\text{C}$  and  $\Theta = 120 \text{ }^\circ\text{C}$



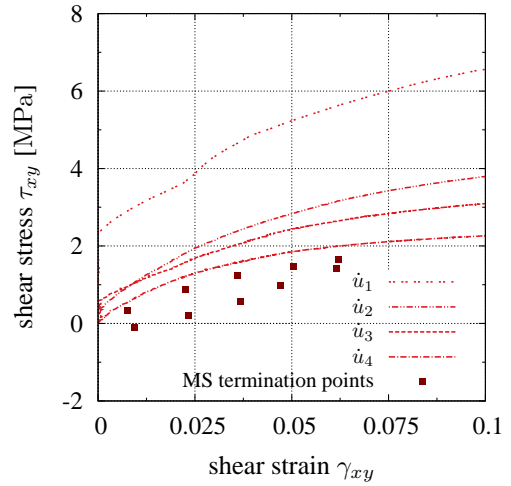
(a) Shear stress vs. shear strain at  $\Theta = -10\text{ }^{\circ}\text{C}$



(b) Shear stress vs. shear strain at  $\Theta = 20\text{ }^{\circ}\text{C}$



(c) Shear stress vs. shear strain at  $\Theta = 50\text{ }^{\circ}\text{C}$



(d) Shear stress vs. shear strain at  $\Theta = 120\text{ }^{\circ}\text{C}$

Figure 28: Comparison between monotonic shear tests and end-points of multi-step shear tests at temperatures  $\Theta = -10\text{ }^{\circ}\text{C}$ ,  $\Theta = 20\text{ }^{\circ}\text{C}$ ,  $\Theta = 50\text{ }^{\circ}\text{C}$ ,  $\Theta = 120\text{ }^{\circ}\text{C}$  ( $\dot{u}_1 = 1\text{ mm s}^{-1}$ ,  $\dot{u}_2 = 10^{-1}\text{ mm s}^{-1}$ ,  $\dot{u}_3 = 10^{-2}\text{ mm s}^{-1}$ ,  $\dot{u}_4 = 10^{-3}\text{ mm s}^{-1}$ )

We present an extensive experimental campaign focusing on a thermo-plastic copolymer of PP/PE. The influence of the displacement-rate and of the temperature is investigated by means of tensile and shear tests with thin foils, while the strains are measured by means of a DIC-system. It is necessary to perform full-field measurements like this since the material shows localization-effects beyond a certain deformation. Following the tests, the localization zone is investigated in respect of a locally homogeneous deformation zone, in order to determine the strain state. Based on the uniaxial tensile state and the information provided by the DIC-system, we also assume a homogeneous stress state in this zone. This, however, is not applicable in the shear tests, so we restrict our investigations to the small strain case for shear.

Uniaxial and multi-step relaxation tests are carried out within large deformations, at four different displacement-rates and four different temperatures. Furthermore, the small deformation range is also investigated at room temperature by means of strain-controlled uniaxial and multi-step relaxation tests, whereas the loading-unloading behavior is addressed additionally. Shear tests, including multi-step tests, are performed within the small deformation range at the same displacement-rates and temperatures considered in the case of tensile tests. By observing the lateral stretch-axial stretch behavior, we are also able to show that the theoretical assumption of incompressibility cannot be considered for the investigated thermo-plastic. Within the large deformation range PP/PE shows localiza-

tion phenomena and a non-linear development of the stretches over the time. The stress-stretch behavior in terms of yield stress, strain softening and strain hardening is found to be rate-dependent and temperature-dependent. Particularly, the stress magnitude increases with the loading rate and decreases with the increase of the temperature - as expected. Within the small deformation range, the PP/PE-copolymer does not show macroscopic phenomena of necking. Nevertheless, pronounced irreversible deformations remain in the material after the tests. The small deformation range, in which the study of the Poisson ratio is added, is also characterized by the rate-dependence and the temperature-dependence. The internal equilibrium state is estimated by considering the termination points of relaxation of the multi-step relaxation tests. The equilibrium stress state is found to be temperature-dependent. Furthermore, the temperature has influence on the development of the necking and the strain distribution within this area.

A three-rail shear tool was developed to study the shear behavior. Except from the edge effects present in a small area around the free edges of the specimens, the distribution of the shear strain is quite homogeneous within the specimens tested in the small strain range. Again, the shear stress-shear strain behavior shows rate- and temperature-dependence - and the amount of shear softening due to the temperature, is approximately the same in all the considered test rates. The equilibrium curve describing the shear stresses shows a decrease in width with an increase of temperature.

## Acknowledgements

We gratefully acknowledge the financial support provided by the German Research Foundation (DFG, grant no. HA2024/12-1). Furthermore, we would like to thank the Institute of Polymer Materials and Plastics Engineering for performing the DSC- and DMA-analysis of the material. Apart from this, Professor Heinz Palkowski and Mohammed Harhash (Institute of Metallurgy) are gratefully acknowledged for many discussions on the subject. Both institutes are located at the Clausthal University of Technology. Furthermore, we give many thanks to both the Clausthal Center of Materials Technology as well as Rose Rogin Gilbert for help in preparing the manuscript.

## Appendix

### A Stretch and Stress Determination

In the localization area we assume a homogeneous deformation state represented by the deformation gradient

$$\mathbf{F} = \text{Grad } \vec{\chi}_R(\vec{X}, t) = \begin{bmatrix} \lambda_x & 0 & 0 \\ 0 & \lambda_y & 0 \\ 0 & 0 & \lambda_z \end{bmatrix} \vec{e}_i \otimes \vec{e}_j, \quad (1)$$

where  $\vec{x} = \vec{\chi}_R(\vec{X}, t) = \lambda_x X \vec{e}_x + \lambda_y Y \vec{e}_y + \lambda_z Z \vec{e}_z$  defines the motion of the material point  $\vec{X}$  at the time  $t$ . The axial stretch  $\lambda_y(t)$  and the lateral stretch  $\lambda_x(t)$  are measured by the DIC-system. Moreover, we assume the same stretch in the thickness direction as in width direction  $\lambda_z(t) = \lambda_x(t)$ . Accordingly, the volumetric behavior can be determined,  $\det \mathbf{F} = \lambda_y \lambda_x^2$ . For more details concerning non-linear kinematics, see, for example, (Haupt, 2002). The stretch  $\lambda_y$  can be interpreted as the ratio of current and initial length  $\lambda_y = L/L_0$ , respectively, within a homogeneously deformed region. The same holds for the lateral directions  $\lambda_x = B/B_0$  and  $\lambda_z = D/D_0$ . For the specimen in Fig. 1 we have  $B_0 = 6$  mm and  $D_0 = 0.6$  mm. In engineering application the following strain measures are of principal interest: logarithmic strains, engineering strains and Green-Lagrange strains,  $\mathbf{E}^{(0)} = \ln \mathbf{U}$ ,  $\mathbf{E}^{(1)} = \mathbf{U} - \mathbf{I}$ ,  $\mathbf{E}^{(2)} = \frac{1}{2}(\mathbf{U}^2 - \mathbf{I})$ , where  $\mathbf{U}$  is the right stretch tensor of the polar decomposition of the deformation gradient  $\mathbf{F} = \mathbf{R}\mathbf{U}$ . For a uniaxial tensile case  $\mathbf{R} = \mathbf{I}$ , we identify the strains in axial direction  $\varepsilon_{yy}^{(0)} = \ln \lambda_y$ ,  $\varepsilon_{yy}^{(1)} = \lambda_y - 1$ ,  $\varepsilon_{yy}^{(2)} = (\lambda_y^2 - 1)/2$ . To minimize the amount of representation, we present all figures in stretches.

The cross-section in the initial state is  $A_0 = B_0 D_0$ . To determine the Cauchy-stresses (true stresses), we need the current cross section,  $A = BD$ . Using the relations  $B = \lambda_x B_0$  and  $D = \lambda_z D_0 = \lambda_x D_0$ , we obtain  $A = A_0 \lambda_x^2$ , i.e. the Cauchy stress (true stress) reads  $T_{yy} = F/A = F/(A_0 \lambda_x^2) = T_{Ryy}/\lambda_x^2$ , applying the 1st Piola-Kirchhoff stress (engineering stress)  $T_{Ryy} = F/A_0$ . This relation can be obtained using the relation  $\mathbf{T} = (\det \mathbf{F})^{-1} \mathbf{F} \mathbf{T}_R^T$  with  $\mathbf{T}_R = T_{Ryy} \vec{e}_y \otimes \vec{e}_y$ , i.e.  $T_{yy} = T_{Ryy}/\lambda_x^2$  with  $\det \mathbf{F} = \lambda_y \lambda_x^2$ .

## B Repeatability

In order to verify the closeness of the experimental results, we performed six uniaxial monotonic tensile tests at a displacement-rate  $\dot{u}$  of  $10^{-1}\text{mm s}^{-1}$  and a constant temperature of  $\Theta = 20^\circ\text{C}$ . Here, a thermal chamber serves to maintain these conditions. The experiments were performed in the same location, by the same observer and with the same measuring instruments and conditions. Also, the experiments were repeated in a short period of time. Thus, the notion of repeatability seemed to be more appropriate for the present investigation than the notion of reproducibility, see (Feinberg, 1995) for a detailed discussion. The results of the tests are presented in terms of 1st Piola-Kirchhoff and Cauchy stresses versus the vertical stretch  $\lambda_y$  in Fig. 29(a) and Fig. 29(b). Additionally, we

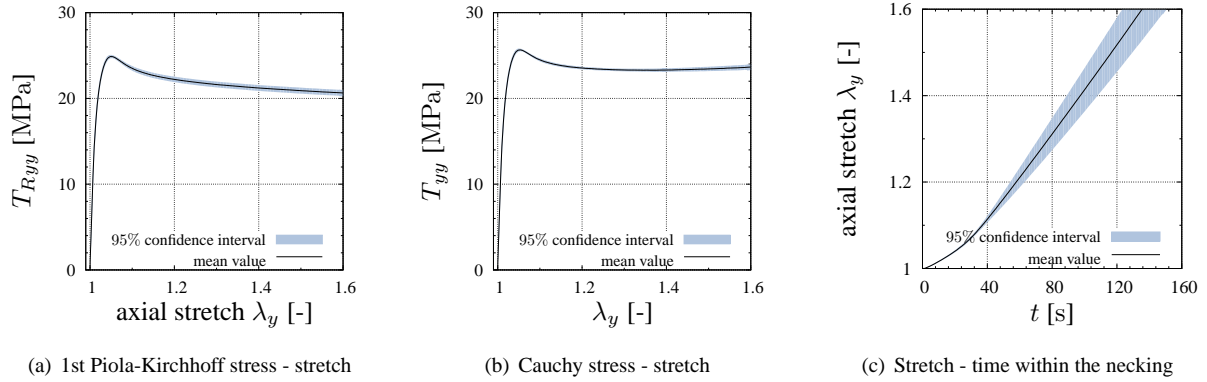


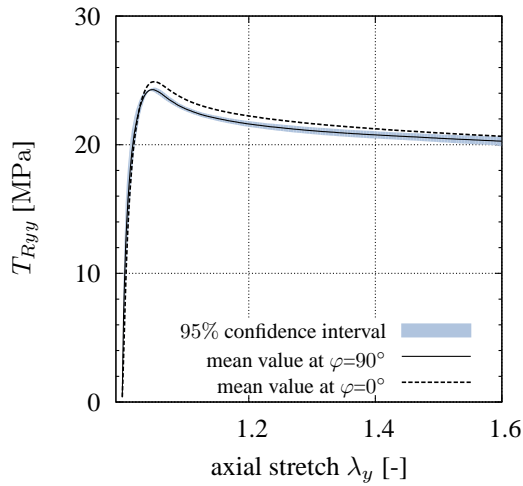
Figure 29: Repeatability of the tests at  $\dot{u} = 10^{-1}\text{mm s}^{-1}$  (6 tests)

computed the mean values of the vertical component of the stresses  $\bar{T}_{Ryy}$  and  $\bar{T}_{yy}$ , and their standard deviation. Two different aspects arise from this analysis. The first issue concerns the standard deviation of the experiments, which shows a peak value within the small deformation range and lower values ( $\approx 0.3$  MPa) within the large deformation range, i.e. after the formation of the necking. Indeed, the diagrams show that the neck does not start at the same moment for all the specimens, even if the setup and the prescribed displacement-rate  $\dot{u}$  are the same for all the considered tests. Nevertheless, the overall stress-stretch behavior is the same after the formation of the necking. Such a different initiation of necking is generally imputed to the initial imperfections of the specimens' shape and local material properties without having influence of the final overall response, see (Wu and van der Giessen, 1995).

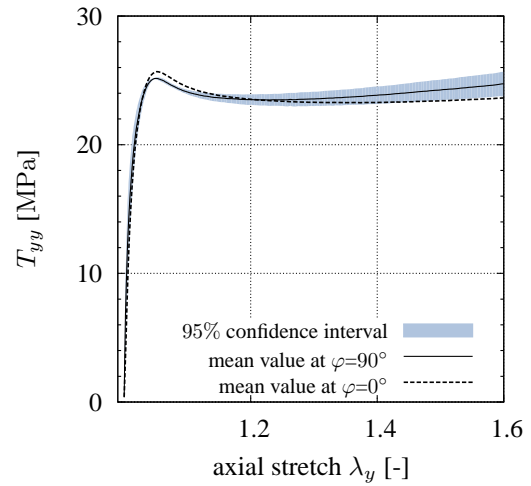
The second arising aspect concerns higher values of stresses in test number four, with respect to the mean value. The explanation can be found by analyzing the behavior during the time of the axial stretch  $\lambda_y$  evaluated within the necking area. Fig. 29(c) illustrates a comparison between the local strain-rates of the tests, and it shows that the stretch-time behavior deviates from other tests. This is due to a faster "local-rate" within the necking zone, as detected by the DIC-system. Consequently, higher values of stresses are to be found for this specimen. In the following - considering this last aspect and the present results - we assume repeatability of the entire experimental campaign and the strain evaluation procedure.

## C Investigation on Anisotropy

In order to investigate whether the material shows any anisotropic behavior, three isothermal monotonic tensile experiments were performed with specimens that were cut out of the foil in the direction  $\varphi = 90^\circ$  orthogonal to the extrusion's direction,  $\varphi = 0^\circ$ . They were tested at a constant temperature  $\Theta = 20^\circ\text{C}$  and a displacement-rate  $\dot{u} = 10^{-1}\text{mm s}^{-1}$  of the traverse. Fig. 30(a) and Fig. 30(b) show the comparison between the monotonic tensile tests, performed with the specimens extracted at  $\varphi = 90^\circ$  and the mean value of the tests performed with the specimens extracted at  $\varphi = 0^\circ$ , at the same displacement-rate and temperature. A comparison in terms of the 1st Piola-Kirchhoff stress  $T_{Ryy}$  and the axial stretch  $\lambda_y$  shows that both the yield stress as well as the softening behavior of the tests lie within the same range of values of the corresponding tests of specimens in extrusion direction. For the Cauchy stress  $T_{yy}$  versus the axial stretch  $\lambda_y$ , the yield stresses lie within the range of values of the corresponding tests in extrusion direction, while the hardening behavior turns out to be more pronounced for two of the tests. This is mainly because of the lateral stretch  $\lambda_x$ . Concerning the main effects of the material



(a) 1st Piola-Kirchhoff stress-axial stretch diagram



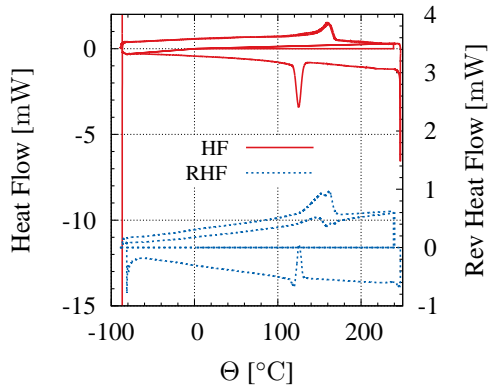
(b) Cauchy stress-axial stretch diagram

Figure 30: Investigation of anisotropic behavior

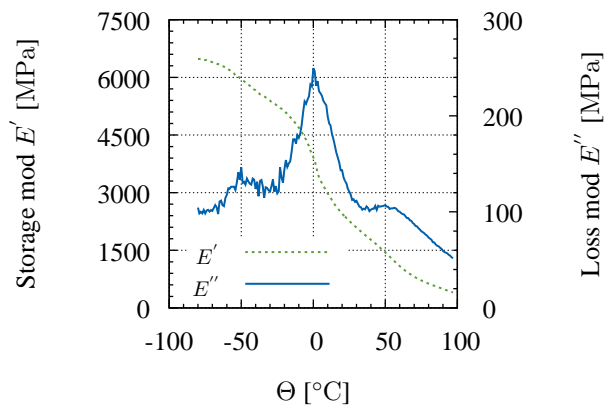
properties, we restrict our investigations to the extrusion direction,  $\varphi = 0^\circ$ , i.e. we assume isotropic material behavior.

#### D Thermal Characterization

The DSC-analyses were performed at decreasing periods of 90 s, 60 s and 40 s and the DMA-analyses were performed at two different frequencies of 10 Hz and 1 Hz. Fig. 31 shows a DSC-analysis performed at a period of 60 s



(a) DSC-analysis at a period of 60 s



(b) DMA-analysis at a frequency of 1 Hz

Figure 31: Thermal characterization of PP/PE using DSC and DMA

and a DMA-analysis performed at a frequency of 1 Hz.

#### References

- Argon, A. S.: A theory for the low-temperature plastic deformation of glassy polymers. *Philosophical Magazine*, 28, (1973), 839–865.
- Arruda, E. M.; Boyce, M. C.; Jayachandran, R.: Effects of strain rate temperature and thermomechanical coupling on the finite strain deformation of glassy polymers. *Mechanics of Materials*, 19, (1995), 193–212.
- ASTM D4255/D4255M-15a: Standard Test Method for In-Plane Shear Properties of Polymer Matrix

- Composite Materials by the Rail Shear Method. ASTM International, West Conshohocken, PA (2015), DOI:10.1520/D4255\_D4255M-15A, www.astm.org.
- ASTM D5379/D5379M-12: Standard Test Method for Shear Properties of Composite Materials by the V-Notched Beam Method. ASTM International, West Conshohocken, PA (2012), DOI:10.1520/D5379\_D5379M-12, www.astm.org.
- ASTM D7078/D7078M-12: Standard Test Method for In-Plane Shear Properties of Polymer Matrix Composite Materials by the Rail Shear Method. ASTM International, West Conshohocken, PA (2012), DOI: 10.1520/D7078\_D7078M-12, www.astm.org.
- Bowden, P.: The Yield Behaviour of Glassy Polymers. In: R. Haward, ed., *The Physics of Glassy Polymers*, pages 279–339, Springer Netherlands (1973).
- Daiyan, H.; Andreassen, E.; Grytten, F.; Osnes, H.; Gaarder, R. H.: Shear testing of polypropylene materials analysed by digital image correlation and numerical simulations. *Experimental Mechanics*, 52, (2012), 1355–1369.
- De Almeida, O.; Lagattu, F.; Brillaud, J.: Analysis by a 3D DIC technique of volumetric deformation gradients: Application to polypropylene/EPR/talc composites. *Composites Part A: Applied Science and Manufacturing*, 39, 8, (2008), 1210–1217.
- Delhaye, V.; Clausen, A. H.; Moussy, F.; Hopperstad, O. S.; Othman, R.: Mechanical response and microstructure investigation of a mineral and rubber modified polypropylene. *Polymer Testing*, 29, 7, (2010), 793–802.
- DIN EN ISO 527-3:2003-07: Plastics - Determination of tensile properties - Part 3: Test conditions for films and sheets. Beuth Verlag GmbH, Berlin (2010), www.beuth.de.
- Drozdov, A. D.: Volume changes in glassy polymers. *Archive of Applied Mechanics*, 68, 10, (1998), 689–710.
- Drozdov, A. D.: Mullins' effect in semicrystalline polymers. *International Journal of Solids and Structures*, 46, (2009), 3336–3345.
- Drozdov, A. D.; Christiansen, J. d.: Cyclic viscoplasticity of high-density polyethylene: Experiments and modeling. *Computational Materials Science*, 39, (2007), 465–480.
- Drozdov, A. D.; Christiansen, J. d.; Klitkou, R.; Potarniche, C. G.: Viscoelasticity and viscoplasticity of polypropylene/polyethylene blends. *International Journal of Solids and Structures*, 47, (2010), 2498–2507.
- Ehrenstein, G. W.; Riedel, G.; Trawiel, P.: *Thermal Analysis of Plastics*. Carl Hanser Verlag GmbH & Co. KG, Munich (2004).
- Feinberg, M.: Basics of interlaboratory studies: the trends in the new ISO 5725 standard edition. *TrAC Trends in Analytical Chemistry*, 14, (1995), 450–457.
- GOM: *Aramis – User Manual: The basics of strain*. GOM – Gesellschaft für optische Messtechnik, Braunschweig, Germany (2011).
- Grytten, F.; Daiyan, H.; Polanco-Loria, M.; Dumoulin, S.: Use of digital image correlation to measure large-strain tensile properties of ductile thermoplastics. *Polymer Testing*, 28, 6, (2009), 653–660.
- G'Sell, C.; Bai, S.-L.; Hiver, J.-M.: Polypropylene/polyamide 6/polyethylene–octene elastomer blends. Part 2: volume dilatation during plastic deformation under uniaxial tension. *Polymer*, 45, (2004), 5785–5792.
- G'Sell, C.; Boni, S.: Application of the plane simple shear test for determination of the plastic behaviour of solid polymers at large strains. *Journal of Materials Science*, 18, (1983), 903–918.
- G'Sell, C.; Hiver, J. M.; Dahoun, A.: Experimental characterization of deformation damage in solid polymers under tension, and its interrelation with necking. *International Journal of Solids and Structures*, 39, (2002), 3857–3872.
- G'Sell, C.; Hiver, J. M.; Dahoun, A.; Souhai, A.: Video-controlled tensile testing of polymers and metals beyond the necking point. *Journal of Materials Science*, 27, (1992), 5031–5039.
- G'Sell, C.; Jonas, J. J.: Determination of the plastic behaviour of solid polymers at constant true strain rate. *Journal of Materials Science*, 14, (1979), 583–591.

- G'Sell, C.; Jonas, J. J.: Yield and transient effects during the plastic deformation of solid polymers. *Journal of Materials Science*, 16, (1981), 1956–1974.
- Hartmann, S.: A thermomechanically consistent constitutive model for polyoxymethylene: experiments, material modeling and computation. *Archive of Applied Mechanics*, 76, (2006), 349–366.
- Haupt, P.: *Continuum Mechanics and Theory of Materials*. Springer, Berlin, 2 edn. (2002).
- Haupt, P.; Lion, A.: Experimental identification and mathematical modelling of viscoplastic material behavior. *Journal of Continuum Mechanics and Thermodynamics*, 7, (1995), 73–96.
- Haupt, P.; Sedlan, K.: Viscoplasticity of elastomeric materials. experimental facts and constitutive modelling. *Archive of Applied Mechanics*, 71, (2001), 89–109.
- Haward, R. N.; Young, R. J.: *The physics of glassy polymers*. Springer Science & Business Media (1997).
- Iosipescu, N.: New accurate procedure for single shear testing of metals. *Journal of Materials*, 2, 3, (1967), 537–566.
- Lange, G.; Carradò, A.; Palkowski, H.: Tailored sandwich structures in the focus of research. *Materials and Manufacturing Processes*, 24, (2009), 1150–1154.
- Lee, S.; Munro, M.: Evaluation of in-plane shear test methods for advanced composite materials by the decision analysis technique. *Composites*, 17, (1986), 13–22.
- Liu, M. C. M.; Krempl, E.: A uniaxial viscoplastic model based on total strain and overstress. *Journal of the Mechanics and Physics of Solids*, 27, (1979), 377–391.
- Lovinger, A. J.; Williams, M. L.: Tensile properties and morphology of blends of polyethylene and polypropylene. *Journal of Applied Polymer Science*, 25, (1980), 1703–1713.
- Maher, J. W.; Haward, R. N.; Hay, J. N.: Study of the thermal effects in the necking of polymer with the use of an infrared camera. *Journal of Polymer Science*, 18, (1980), 2169–2179.
- Maurel-Pantel, A.; Baquet, E.; Bikard, J.; Bouvard, J. L.; Billon, N.: A thermo-mechanical large deformation constitutive model for polymers based on material network description: Application to a semi-crystalline polyamide 66. *International Journal of Plasticity*, 67, (2015), 102–126.
- Palkowski, H.; Sokolova, O. A.; Carradò, A.: Sandwich materials. In: *Encyclopedia of Automotive Engineering*, pages 1 – 17, John Wiley & Sons, Ltd (2013).
- Pandini, S.; Pegoretti, A.: Time and temperature effects on Poisson's ratio of poly(butylene terephthalate). *Express Polymer Letters*, 5, 8, (2011), 685–697.
- Petrynyuk, J. S.; Priadilova, O. V.; Levin, V. M.; Ledneva, O. A.; Popov, A. A.: Structure and elastic properties of immiscible LDPE-PP blends dependence on composition. In: *Symposium I -Nanomaterials for Structural Applications*, vol. 740 of *MRS Proceedings* (2002).
- Raghava, R.; Caddell, R.; Yeh, G.: The macroscopic yield behaviour of polymers. *Journal of Materials Science*, 8, 2, (1973), 225–232.
- Rouault, T.; Bouvet, C.; Nègre, V.; Rauch, P.: Reversible rail shear apparatus applied to the study of woven laminate shear behavior. *Experimental Mechanics*, 53, (2013), 1437–1448.
- Sedlan, K.: *Inelastisches Materialverhalten von Elastomerwerkstoffen: Experimentelle Untersuchung und Modellbildung*. Doctoral thesis, Institute of Mechanics, University of Kassel (2000), report No. 2/2001.
- Sleuwen, J. K.: *Entwicklung und Konstruktion eines Werkzeugs zum Durchführen von Scherversuchen an dünnen Polymerproben*. B. Sc.-thesis, TU Clausthal, Germany (2014).
- Sutton, M. A.; Orteu, J.-J.; Schreier, H. W.: *Image correlation for shape, motion and deformation measurements*. Springer, New York (2009).
- Ward, I.: Review: The yield behaviour of polymers. *Journal of Materials Science*, 6, 11, (1971), 1397–1417.
- Ward, I. M.; Hadley, D. W.: *An introduction to the mechanical properties of solid polymers*. John Wiley & Sons Ltd.; John Wiley & Sons, Inc. (1993).

- Whitney, J. M.; Stansbarger, D. L.; Howell, H. B.: Analysis of the Rail Shear Test-Applications and Limitations. *Journal of Composite Materials*, 5, 1, (1971), 24–34.
- Wu, P.; van der Giessen, E.: On neck propagation in amorphous glassy polymers under plane strain tension. *International Journal of Plasticity*, 11, 3, (1995), 211–235.
- Yin, Q.; Zillmann, B.; Suttner, S.; Gerstein, G.; Biasutti, M.; Tekkaya, A. E.; Wagner, M. F. X.; Merklein, M.; Schaper, M.; Halle, T.; Brosius, A.: An experimental and numerical investigation of different shear test configurations for sheet metal characterization. *Internal Journal of Solids and Structures*, 51, (2014), 1066–1074.
- Zaroulis, J. S.; Boyce, M. C.: Temperature, strain rate, and strain state dependence of the evolution in mechanical behaviour and structure of poly(ethylene terephthalate) with finite strain deformation. *Polymer*, 38, (1997), 1303–1315.
- Zhou, Y.; Mallick, P. K.: Effects of temperature and strain rate on the tensile behavior of unfilled and talc-filled polypropylene. Part I: Experiments. *Polymer Engineering & Science*, 42, 12, (2002), 2449–2460.

---

*Address:* Prof. Dr.-Ing. Stefan Hartmann, Institute of Applied Mechanics, Clausthal University of Technology, Adolph-Roemer-Str. 2a, 38678 Clausthal-Zellerfeld, Germany  
email: stefan.hartmann@tu-clausthal.de